375
9/21
Don't Recycle 120
C-41
A+B Formal
DWR-1548

AI-AEC-12977

MASTER

AEROSOL MODELING OF HYPOTHETICAL LMFBR ACCIDENTS

AEC Research and Development Report

Atomics International
North American Rockwell

P.O. Box 309
Canoga Park, California 91304

DISTRIBUTION OF THIS DOCUMENT IS UNLIMITED

DISCLAIMER

This report was prepared as an account of work sponsored by an agency of the United States Government. Neither the United States Government nor any agency Thereof, nor any of their employees, makes any warranty, express or implied, or assumes any legal liability or responsibility for the accuracy, completeness, or usefulness of any information, apparatus, product, or process disclosed, or represents that its use would not infringe privately owned rights. Reference herein to any specific commercial product, process, or service by trade name, trademark, manufacturer, or otherwise does not necessarily constitute or imply its endorsement, recommendation, or favoring by the United States Government or any agency thereof. The views and opinions of authors expressed herein do not necessarily state or reflect those of the United States Government or any agency thereof.

DISCLAIMER

Portions of this document may be illegible in electronic image products. Images are produced from the best available original document.

LEGAL NOTICE

This report was prepared as an account of Government sponsored work. Neither the United States, nor the Commission, nor any person acting on behalf of the Commission:

A. Makes any warranty or representation, express or implied, with respect to the accuracy, completeness, or usefulness of the information contained in this report, or that the use of any information, apparatus, method, or process disclosed in this report may not infringe privately owned rights; or

B. Assumes any liabilities with respect to the use of, or for damages resulting from the use of information, apparatus, method, or process disclosed in this report.

As used in the above, "person acting on behalf of the Commission" includes any employee or contractor of the Commission, or employee of such contractor, to the extent that such employee or contractor of the Commission, or employee of such contractor prepares, disseminates, or provides access to, any information pursuant to his employment or contract with the Commission, or his employment with such contractor.

Printed in the United States of America
Available from
Clearinghouse for Federal Scientific and Technical Information
National Bureau of Standards, U.S. Department of Commerce
Springfield, Virginia 22151
Price: Printed Copy $3.00; Microfiche $0.65

AI-AEC-12977
HEALTH AND SAFETY

AEROSOL MODELING OF HYPOTHETICAL LMFBR ACCIDENTS

By

R. L. KOONTZ
L. BAURMASH
M. A. GREENFIELD
C. T. NELSON
D. F. HAUSKNECHT
E. U. VAUGHAN
M. SILBERBERG
H. A. MOREWITZ

LEGAL NOTICE

This report was prepared as an account of Government sponsored work. Neither the United States, nor the Commission, nor any person acting on behalf of the Commission:

A. Makes any warranty or representation, expressed or implied, with respect to the accuracy, completeness, or usefulness of the information contained in this report, or that the use of any information, apparatus, method, or process disclosed in this report may not infringe privately owned rights; or

B. Assumes any liabilities with respect to the use of, or for damages resulting from the use of any information, apparatus, method, or process disclosed in this report.

As used in the above, "person acting on behalf of the Commission" includes any employee or contractor of the Commission, or employee of such contractor, to the extent that such employee or contractor of the Commission, or employee of such contractor prepares, disseminates, or provides access to, any information pursuant to his employment or contract with the Commission, or his employment with such contractor.

Atomics International
North American Rockwell

P.O. Box 309
Canoga Park, California 91304

CONTRACT: AT(04-3)-701
ISSUED: AUGUST 31, 1970

DISTRIBUTION OF THIS DOCUMENT IS UNLIMITED

DISTRIBUTION

This report has been distributed according to the category "Health and Safety" as given in the Standard Distribution for Unclassified Scientific and Technical Reports, TID-4500.

CONTENTS

TABLES

FIGURES

FIGURES

ABSTRACT

The report represents a description of an aerosol model (HAA-3) which is consistent with existing experimental data and which can be defended for use in design or licensing of LMFBR's. Comparison of theory and experiments performed in a vessel whose height is typical of LMFBR inner containment are presented for four independent time varying parameters. A detailed justification of the model and the application of various model assumptions and parameters to accident conditions is described. A description is presented of additional aerosol behavior characteristics suggested by experimental data or analytical considerations, which are not completely resolved. The potential effects of these characteristics are evaluated by parameter sensitivity evaluation with the model.

I. PROBLEM BACKGROUND

Aerosol research studies sponsored by the AEC-RDT have been in progress at Atomics International for several years. The program is directed toward the characterization of the aerosols produced during sodium fires and other postulated Liquid Metal Fast Breeder Reactor (LMFBR) accidents, particularly the explosive disassembly regime, e.g., design basis accident (DBA). One of the key objectives of the AI program has been to develop analytical methods and tools for predicting aerosol transport following various accidents. As the program has progressed through various experimental and analytical stages, the analytical methods which evolved have been improved with respect to engineering, applicability, and accuracy, and also, level of confidence. The AI aerosol program has progressed to the point where the present theoretical aerosol model (HAA-3 code) has been extended to compute high mass concentration cases. Since these calculations have been tested with reasonable success against experiments in a 30-ft-tall test chamber (the approximate height of primary vaults for a typical LMFBR), HAA-3 can be confidently used in evaluations of potential releases from similar sized structures.

The report presents a description of the HAA-3 aerosol model which is consistent with existing experimental data and can be used as design input in establishing the capability of containment-related design features of LMFBR's. A detailed justification of the model and the application of various model assumptions and parameters to accident conditions is described. A description is presented of additional aerosol behavior characteristics suggested by experimental data or analytical considerations, which are not completely resolved. The potential effects of these characteristics are discussed in detail.

THIS PAGE

WAS INTENTIONALLY

LEFT BLANK

II. REVIEW OF SOME OF THE RELEVANT AEROSOL LITERATURE

Smoluchowski first formulated the collision dynamics of aerosols. In a series of papers,[1-3] he described the possibility of coagulation or agglomeration of particles colliding as a result of Brownian motion as well as shear flow. The initial derivation was for monosize distribution of particles but in subsequent work he derived the kinetic equations for a discrete polydisperse distribution of particles and obtained an approximate solution for the initial stage of coagulation. Muller[4,5] formulated the integrodifferential equation for a continuous distribution. However, as was noted much later by Zebel,[6] a factor inside one of the integrals has been neglected. Independent of Muller's work, Schumann[7] obtained the fundamental equation for coagulation of a continuous polydisperse population. He was also able to solve this equation by assuming a collision process which was independent of particle size. His solution agreed with size distributions of fog particles measured by Houghton and Radford.[8] Melzak[9] following a similar approach showed agreement with the smaller end of the raindrop spectrum measured by Marshall and Palmer.[10] Agreement in both of these cases is a verification of the approximation that for a narrow (approximately monosize) distribution of particles whose size is greater than the mean free path of the gas molecules, the collision rate due to Brownian movement is independent of particle size.

Zebel[6] was apparently the first to report time dependent aerosol distributions obtained from the fundamental equation by computer evaluation. He demonstrated that numerical evaluation of the aerosol equation, using a measured distribution as an initial condition, could predict the subsequent behavior of the suspension.

Saffman and Turner[11] contributed significantly to the theory of the collision process by formulating the collision probability due to gravity and turbulence. Two distinct affects of turbulence were recognized as contributing to collisions. Turbulent shear and turbulent accelerations each gave rise to collisions. They applied the theory of raindrop growth in clouds, but no extensive calculations were made.

By means of similarity hypothesis, Friedlander[12] and co-workers developed and experimentally tested mathematical expressions for a similarity theory leading to a "self-preserving" or asymptotic distribution. In Friedlander's early work, a quasi-steady-state distribution for natural atmospheric aerosols was conceptualized. The distribution was evolved as a result of a steady process wherein small particles arising from various sources (condensation, sea spray, man-made generators, etc.) entered the lower end of the spectrum. The small particles grow by coagulation due to Brownian motion, and finally were removed at the upper end of the spectrum by sedimentation. By dimensional analysis an expression was obtained which explained to a degree the similar shape of atmospheric aerosol distributions observed in various parts of the world. Later, the similarity arguments were extended to introduce the "self-preserving hypothesis." This theory assumes that there exist certain classes of asymptotic solutions to the kinetic equations for coagulating aerosols which are "universal" and are independent of the initial distribution. The initial model for self-preservation was applied to coagulation of particles by Brownian motion in a closed vessel without removal of mass. The time-dependent model included approximate solutions for the upper and lower ends of the spectrum with a numerical evaluation of the entire spectrum. Independently and earlier, Todes[13] had studied the asymptotic behavior with only Brownian motion considered, and obtained a solution analogous to that of Friedlander and colleagues.

Hidy[14] and co-workers reviewed the theory of particles colliding due to Brownian motion and noted the attempts to develop a suitable formulation for the transition between the collision rate for molecules (kinetic theory of gases) and the formulation of Smoluchowski for particles much larger than the mean free path of the gas molecules. They also carried out numerical evaluations of the fundamental equation (with Brownian motion as the coagulation mechanism) and substantiated Friedlander's self-preserving spectrum hypothesis.

Takahashi and Kasahara[15] computed many cases from the basic equation and included coagulation due to Brownian motion, gravity, and turbulence. They also noted that for agglomeration due to Brownian motion only, the early (1940) analytical solution of Schumann[7] gives the identical time-dependent distribution of Friedlander (1966).

The effects of radioactivity on the coagulation rates were observed by Rosinski, Werle, and Nagamoto.[16] They observed that a high degree of radioactivity gave a twenty-fold increase in the initial coagulation rate. A minor effect was observed when inactive and slightly active aerosols were mixed. Scavenging of radioactive particles by the addition of inactive aerosols was also studied.

Existence and uniqueness of the solutions of both the discrete and continuous formulations were proven by McLeod.[17] These were limited proofs in that only simple dependence of collision probability was assumed. Several analytical results were obtained by Martynov and Bakanov,[18] but they are mainly of theoretical interest.

An interesting practical application of coagulation theory to hydrosols was made by Fair and Gemmell.[19] They quantified the idea of Camp[20] for optimizing the design of coagulation basins for waste disposal. Floc growth in the sheared suspension is restricted by larger particles breaking up due to collisions. They applied Smoluchowski's formulation for growth in a sheared suspension and imposed an upper limit for growth above which particles would fragment. Oscillatory growth patterns were calculated for some combinations of initial concentration and shear rate; and were also observed experimentally.

A model for the formation and dispersion of fallout particles from sea-water-surface nuclear bursts was developed by Huebsch in a series of reports.[21] The theory of collisions of aerosol particles was extended by him to include turbulent agglomeration of particles whose sizes are larger than the scale of the eddies. Agreement of numerical results with measured particles sizes (including "super giant nuclei" of 200 μm diameter and greater) demonstrated that for low yield bursts coagulative growth was due mainly to gravity and for high yield bursts growth was due primarily to turbulence. In the case of low yield bursts, growth of particles is extremely sensitive to atmospheric humidity.

The coagulation of sodium and uranium oxide aerosols have been studied by workers at Atomics International.[22-26] Aerosols were generated in chambers with heights of 6 and 30 ft and measurements of floor and wall deposition rates, air concentration, and particle size distribution as functions of time were obtained. The sodium and sodium oxide aerosols formed nonspherical clumps

while the uranium oxide formed open structure branched chains. Numerical evaluation of the fundamental coagulation model with terms which represent the collisions due to Brownian motion, gravity, and turbulence was accomplished. Terms representing sedimentation and plating on chamber walls were also included in the model. For the smaller chamber, agreement with measurements is good.[24] For a larger test chamber (which allows particles more time to settle) with higher concentrations, the sodium oxide agglomerates grow to large nonspherical clusters with reduced smeared density. For this reason, a correction to the Stokes velocity is required.

Castleman, Horn, and Lindauer[27] have conducted experiments using plutonium and uranium oxides. In addition, they obtained solutions of the fundamental coagulation equation by computerized numerical evaluation. A theoretical formulation of collision efficiency, which considered the idealized hydrodynamic interaction of approaching spheres (although the measured shapes were far from spherical) was included in the gravitational and turbulent collision probability terms. Although good agreement was obtained between their theory and experimental results, it is believed that the experimental design was such (relatively low concentrations and small initial particle size) that gravitational agglomeration would be expected to play a minor role in the coagulation process. Consequently their formulation of the collision efficiency for gravitational agglomeration was not conclusively tested. Collision efficiency is discussed in some detail in Section IV-B-3.

It can be seen from the above discussion that the basic theory of coagulation of particulates has been applied to a wide range of problems by modern computer techniques. The detailed formulation depends on the problem parameters of concern and the computed results have predicted a wide range of experimental situations.

III. DESCRIPTION OF AEROSOL COAGULATION AND DEPOSITION CONCEPTS

A. THE COAGULATION CONSTANT

Coagulation of aerosols is used to describe the process of adhesion of aerosol particles upon contact with one another. When the approach of particles, leading to contact, can only be effected by Brownian movement (diffusion), the process is called thermal coagulation.[1,2]

For the general case of nonequal particles [polydisperse aerosol, Müller[4,5]], the number N_{12} of particle 2 with radius r_2, diffusing in unit time to a fixed particle 1 with radius r_1, follows from the diffusion theory, if r_2 is greater than the mean free path of air.

$$\dot{N}_{12} = 4\pi D_2 r_{12} n(r_2, t) \qquad \ldots(1)$$

where:

$r_{12} = r_1 + r_2$ is the distance between the centers of the two particles at the moment of contact;

D_2 = the diffusion coefficient for the particles of kind 2

$n(r_2, t)$ = the concentration of particles of radius r_2 at time; t, at a distance equal to infinity.

The Brownian movement of both particles has to be taken into account by a summation of the diffusion coefficients. The relative diffusion coefficient of two particles is equal to the sum of the diffusion coefficients of the single particles.

Using the well-known relation between the diffusion coefficient D and the mobility B of a particle

$$D = BkT\,, \qquad \ldots(2)$$

one obtains from Equation 1

$$\dot{N}_{12} = 4\pi(B_1 + B_2)(r_1 + r_2)kTn(r_2, t) \qquad \ldots(3)$$

where k is the Boltzmann constant and T is the absolute temperature.

Introducing a term for the coagulation constant, K_o, where

$$K_o(r_1, r_2) = 4\pi(B_1 + B_2)(r_1 + r_2)kT \ , \qquad \ldots(4)$$

Equation 3 transforms to

$$\dot{N}_{12} = K_o(r_1, r_2)n(r_2, t) \qquad \ldots(5)$$

which means that the number, N_{12}, of particles with radii r_2 adhering to a particle with radius r_1 per unit time at the time t, is equal to the product of the coagulation constant $K_o(r_1, r_2)$ and the particle concentration $n(r_2, t)$.

Note that Equation 1 also represents the condensation rate of r_2, on r_1, if r_1 is large compared to r_2.

The constant K_o has to be corrected for the discontinuity of particle concentration at the surface of the absorbing sphere. The existence of the jump is explained elsewhere.[28] The product of the correction factor and the constant is $K = K_o f$. These values are shown in Table I, while the values for K_o appear in Table II.[28]

Comparing Tables I and II, it is evident that the coagulation constant, K, for very small particles is not due to pure diffusion. On the other hand, the gas kinetic correction factor, f, only slightly influences the value, K_o, for aggregate formation between large and small particles. Small particles are very rapidly scavenged by large ones.

TABLE I

The Coagulation Constant $K(r_1, r_2) = K_o f(10^{-10} cm^3\text{-}sec^{-1})$*

$r_1(\mu)$; $r_2(\mu)$	0.001	0.01	0.1	1.0
0.001	8.78			
0.01	180.2	21.0		
0.1	8845	168.5	11.10	
1.0	178100	2032	35.95	6.44

*Taking into account the gas kinetic correction, f.

TABLE II

Value of the Coagulation Constant $K_o(r_1, r_2)$ $(10^{-10} cm^3 sec^{-1})$*

$r_1(\mu)$; $r_2(\mu)$	0.001	0.01	0.1	1.0
0.001	803.4			
0.01	2232	84		
0.1	20299	234.3	12.68	
1.0	201054	2121	36.69	6.6

*Calculated from diffusion theory

B. BASIC REMOVAL THEORY

Smoluchowski[1, 2] obtained a simple differential equation between the concentration of the total number of particles, n, and the value of K_o, the coagulation constant. The fundamental equation of coagulation becomes

$$\frac{dn}{dt} = -\frac{K_o}{2} n^2. \qquad \ldots(6)$$

The factor 1/2 is necessary so that each aggregate is counted only once. The solution is

$$\frac{1}{n} - \frac{1}{n_o} = \frac{K_o}{2} t \text{ or } n = \frac{n_o}{1 + \frac{K_o}{2} n_o t} = \frac{n_o}{1 + t/t_h} \qquad \ldots(7)$$

where n_o = the initial particle number concentration at time, t = o and the half-value time for the particle number concentration $t_h = 2/K_o n_o$.

Expression 7 for the particle number concentration as a function of time, t, is a good approximation for the size distributions occurring in many aerosols. The increase of the mean particle size, in the course of time reduces the value of K_o (Table II). This is more or less balanced by the increasing polydispersion with its opposite effect.[29]

As the mean particle size increases to sufficiently large values, settling occurs. This causes different size particles to be in relative motion

and to have different falling speeds relative to one another. The latter causes additional collisions which are termed gravitational coagulation.

Settling causes particles to be removed completely from the airborne distribution giving rise to a decrease in the mass concentration. Agglomeration, in contrast, decreases the total number concentration of particles which are airborne.

In all studies performed at AI the environmental conditions in the test chambers can be described as "stirred." This is a condition in which a uniform concentration of particles is maintained throughout the test chamber. In a stirred environment of monosized particles, the rate of decrease of concentration is:

$$dc/dt = -\frac{v_s}{H}\ c \qquad \ldots(8)$$

where

H = height of the chamber (cm)

v_s = settling velocity (cm/sec)

c = concentration (gm/m^3).

The solution to Equation 8 allows one to specify the half time for the mass concentration as

$$T_m = 0.69/(v_s/H) .$$

There are thus two characteristic half times one proportional to the number and the other to the size of the particle, since the velocity is proportional to the radius squared.

The concentration of a cloud of aerosol will decrease as a result of mutual repulsion or attraction depending on whether the system is unipolar or biopolarly charge. If a uniform cloud of unipolar charged particle existed, the total number would decrease due to the migration of the charged particles to the boundaries of the system due to space charge. For small ions Whitby and Liu[30] show that

$$N = \frac{N_o}{3.61 \times 10^{-6} N_o t + 1}$$

where N_o = the initial concentration of ions. Contrast this with the rate of disappearance of neutral particles by agglomeration

$$n = \frac{n_o}{\frac{6 \times 10^{-10}}{2} N_o t + 1} .$$

The decay due to wall deposition (floor, ceiling, and vertical) of uniformly charged aerosols may be considerably higher than for a neutral aerosol which only agglomerates. A discussion of bipolar charged aerosols will be presented in later sections.

THIS PAGE

WAS INTENTIONALLY

LEFT BLANK

IV. THEORETICAL BASIS OF THE MODEL

A. THE GENERAL EQUATIONS

The theoretical basis of the aerosol model is that due to Brownian movement, turbulence, and the different rates of fall of various sized particles under the influence of gravity, collisions between the particles take place and upon collision agglomeration results. There will thus be a gradual increase in the average size of the particles and a reduction in smeared density of the agglomerates constituting the aerosol due to these collisions, and the problem is to determine what the resultant size and mass distribution of the aerosol will be as time increases.

The basic coagulation equation for aerosols having a distribution of particle sizes has the form:

$$\frac{\partial n(v,t)}{\partial t} = A_+(v,t) - A_-(v,t) \qquad \ldots(9)$$

where

$n(v,t)$ = concentration of particles of volume v,

$A_+(v,t)$ = rate of formation of particles of volume v by agglomeration of smaller particles,

$A_-(v,t)$ = rate at which particles of volume v are lost by agglomeration to yield larger particles.

The terms A_+ and A_- are integrals over the various sizes (volumes) of particles that contribute to the processes they respectively represent. They contain the distribution function $n(v,t)$ and also a "coagulation coefficient,"

$$K(v,v'), \qquad \ldots(10)$$

which represents the rate of collision between particles of volumes v and v' if such particles are at unit concentration. Three mechanisms are possible contributors to the collision of the aerosols. All assume an efficiency of one for particle collisions:

1) Brownian Motion

Brownian motion of the aerosol particles arises from their collisions with air molecules which are in thermal motion.

2) Gravity

Particles falling under the influence of gravity will distribute themselves over a range of speeds because of the dependence of the resistance of air on particle size. As a result, coarse particles will tend to sweep past finer ones thereby causing collisions. The coagulation constant is, of course, different than K defined previously.

3) Turbulence

The two ways in which turbulence can cause collisions between adjacent particles are: (1) spatial variations of the turbulent motion causing eddies to collide with one another and thereby producing collisions between the particles entrained in the eddies (shear); and (2) turbulent accelerations of an eddy and the size differences of entrained particles causing them to collide within an eddy.

In both situations, the magnitude of the effect depends on the values of the parameter, ϵ, the rate of energy dissipation per unit mass of suspended material. A more thorough discussion of the relative importance of these three effects is presented in Section IV-B-4 of this report.

For application to reactor safety problems, it is necessary to modify Equation 1 by adding terms that represent two effects not contemplated in the theory for colliding particles.

1) The aerosol production rate must be represented by a source term $S(v,t)$

2) Aerosol particles are removed from the system by fallout, by leakage from the containing vessel or chamber, and by deposition on the walls of the container. This is represented by a removal term $R(v,t)$. With these modifications, the coagulation equation takes the form:

$$\frac{\partial n(v,t)}{\partial t} = A_+(v,t) - A_-(v,t) - R(v,t) + S(v,t). \qquad \ldots(11)$$

This equation now develops in two stages:

1) The removal term $R(v,t)$ is described by a removal coefficient $R(v)$, while the agglomeration terms $A_+(v,t)$ are controlled by the coagulation coefficient $K(v,v')$. The physical processes that contribute to these effects have to be modeled and formulated as contributions to these coefficients, thus making specific the general Equation 11.

2) The specific equation thus obtained must be solved to obtain the size-distribution at all times, $n(v,t)$. The solutions are obtained from computers and more rigorous treatment can be found in the next sections of this report.

The removal processes of primary practical concern are leakage, fallout, and plating. In the model used for the former, the mixture of air and aerosol particles is supposed to escape without change of composition at a rate determined by the nature of the leaks. For site safety analysis this is conservative, since it makes no allowance for deposition of aerosol particles in the channels through which leakage occurs. The fallout model used is that of "stirred settling," in which the spatial variations in composition of the aerosol, due to concentration of larger particles in the lower part of the chamber by their more rapid fall, are assumed to be wiped out by the convection currents set up in the air by heat generated at the floor.

In small chambers, wall deposition is significant. A theory of this effect is therefore needed in the calculations for small chambers, even though it will not contribute appreciably in chambers used to house reactors. The theory used treats the deposition as occurring by Brownian diffusion to the wall through a laminar boundary layer whose thickness is adjusted to give the observed total amount of the deposition. This is in effect a semi-empirical method of subtracting the wall deposition from the other phenomena involved, which are the real objects of the investigation. Its purpose is to derive from the total deposition, the time-dependence of the deposition. Since the deposition increases steadily with time, the latitude within which

its time-dependence can vary is limited, and since the total wall deposition is only about half of the fallout, the error in treating the latter is still smaller. Hence, such a simplified interpolation theory for deposition should be adequate when extrapolations are made to large chambers.

In terms of the number density distribution n(v, t) of the suspended material, the integro-differential equation for the behavior of an heterogenous aerosol is[31]

$$\frac{\partial n(v,t)}{\partial t} = \frac{1}{2}\int_0^v n(v',t)n(v-v',t)F(v',v-v')dv' - n(v,t)\int_0^\infty n(v',t)F(v,v')dv' - R(v)n(v,t) + S(v,t), \quad \ldots (12)$$

where

$v = r^3$, that is, spherical particles are assumed,

r = particle radius,

$F(v, v')$ = normalized collision kernel which gives the probability of collision between two particles of radii, r and r′, due to Brownian motion and due to differences in setting velocities (gravity),

$R(v)$ = removal rate due to settling, wall plating, and leakage, and

$S(v, t)$ = source rate for particles of radius, r.

The first integral represents the rate of production of particles of size, v, due to all collisions between two particles of size, v′ and v - v′. The second integral gives the rate at which particles of size, v, grow to larger sizes due to collisions with particles of size, v′.

The removal rate, R(v), is given by

$$R(v) = G_R v^{2/3}\left[1 + C_1(v)\right] + P_R v^{-1/3}\left[1 + C_1(v)\right] + R_L, \quad \ldots (13)$$

where:

$G_R = \frac{2g\delta}{9h\eta}$, the settling constant,

h = height of chamber $\left(h = \frac{V_c}{A_F}\right)$,

η = viscosity,

δ = density of aerosol material,

g = acceleration due to gravity,

$P_R = \frac{kTA_w}{6\pi\eta\Delta V_c}$, the plating constant,

A_F = area of the floor,

A_w = area of surface for plating,

V_c = volume of chamber,

Δ = distance perpendicular to the wall over which a gradient of the particle density is assumed to exist (Δ is an adjustable parameter required to fit experimental wall plating data),

k = Boltzmann constant, and

T = temperature.

The term containing G_R is the removal rate due to settling; the term containing P_R is the removal rate due to plating. The R_L term is the removal rate due to leakage and is a constant, independent of particle size. Both G_R and P_R are geometry dependent.

B. PARAMETERS NOT DEFINED IN THE GENERAL EQUATION

1. Stokes Correction Factor (α)

Solid aerosol particles have shape, size, configuration, and motion, all varying with time. These variables are reduced to the single one of the size by a series of approximations. These approximations can be considered essential, since the resulting simplified problem is still barely tractable.

The shapes of the aged aerosols are formed by agglomeration and are far too irregular for rigorous treatment, or convenient realistic approximation. They are accordingly approximated as spherical. This procedure requires further study, for while the possibilities are too complex for accurate analysis, they may be too important for complete omission.

Motion is simplified by the steady-state diffusion approximation, which originates with Einstein and Smoluchowski. Each particle is assumed to fall through the air with the terminal velocity imposed by gravity, except for a diffusion from regions of high concentration to regions of low concentration that arises ultimately from a Maxwellian distribution of departures of the velocity from the terminal velocity. The "steady-state" feature is the ignoring of the time to re-establish the assumed conditions when they have been disrupted by a collision and resulting coagulation. The effect of the approximation is that no independent velocity variable need be considered other than V_s.

Stoke's Law was derived for spherical bodies and the more the body deviates from a spherical equivalent the more its velocity deviates from the computed settling velocity. A dynamic shape factor, S, customarily is used to correct the calculated velocity to take into account the nonsphericity of the particle.

The correct equation for the calculation of the Stokes velocity than can be written as

$$V_s = \frac{2 r_e^2 \delta_e g}{9 S \eta} \qquad (16)$$

where

r_e = radius of sphere with the same volume as the particle,
δ_e = effective agglomerate density,
S = dynamic shape factor,

g = gravitational factor, and

η = gas viscosity.

Since it is difficult to separate the effects of smeared density and shape factor on the settling velocity of a particle, most work on shape factors has been performed with solid bodies in the desired shape.[32] Experimental studies of cylinders, parallelepipeds, ellipsoids, and cones with ratios of the height to the diameter of 4.0 show that the shape factor would vary from 1.1 to 1.3. The shape factor for prolate ellipsoids with the ratio of the axes as large as 20 is 2.0. Linear chain agglomerates can be treated as prolate ellipsoids with errors of only a few percent. Experimental studies of linear agglomerates, consisting of glass beads stuck together, show the shape factor increasing from 1.16 to 2.14 as the number of beads are increased from 2 to 8. Flat aggregates of 3 and 7 particles have shape factors of 1.3 and 1.7. Octahedra of 6 particles have a shape factor of 1.3.

Fuchs[33] suggests that the ratio of settling rates oscillates between 0.1 and 0.7 depending on the nature of the packing of the primary particles.

In an experimental study by Stober,[34] the combined effect of shape factor and smeared density was evaluated for aggregates of uniform spheres. He varied the number of basic particles in the agglomerate to eleven and found that the Stokes diameter, D_s, of the aggregate could be defined as

$$D_s = \sqrt[4]{n}\, D$$

where

n = the number of basic particles in the aggregate, and

D = the diameter of the uniform sphere.

Since the equivalent diameter of the agglomerate is

$$D_e = \sqrt[3]{n}\, D ,$$

a computed correction factor, which was validated up to only 11 particles, is:

$$S = \frac{D_e^{\,2}}{D_s^{\,2}} = (n)^{1/6}. \qquad (17)$$

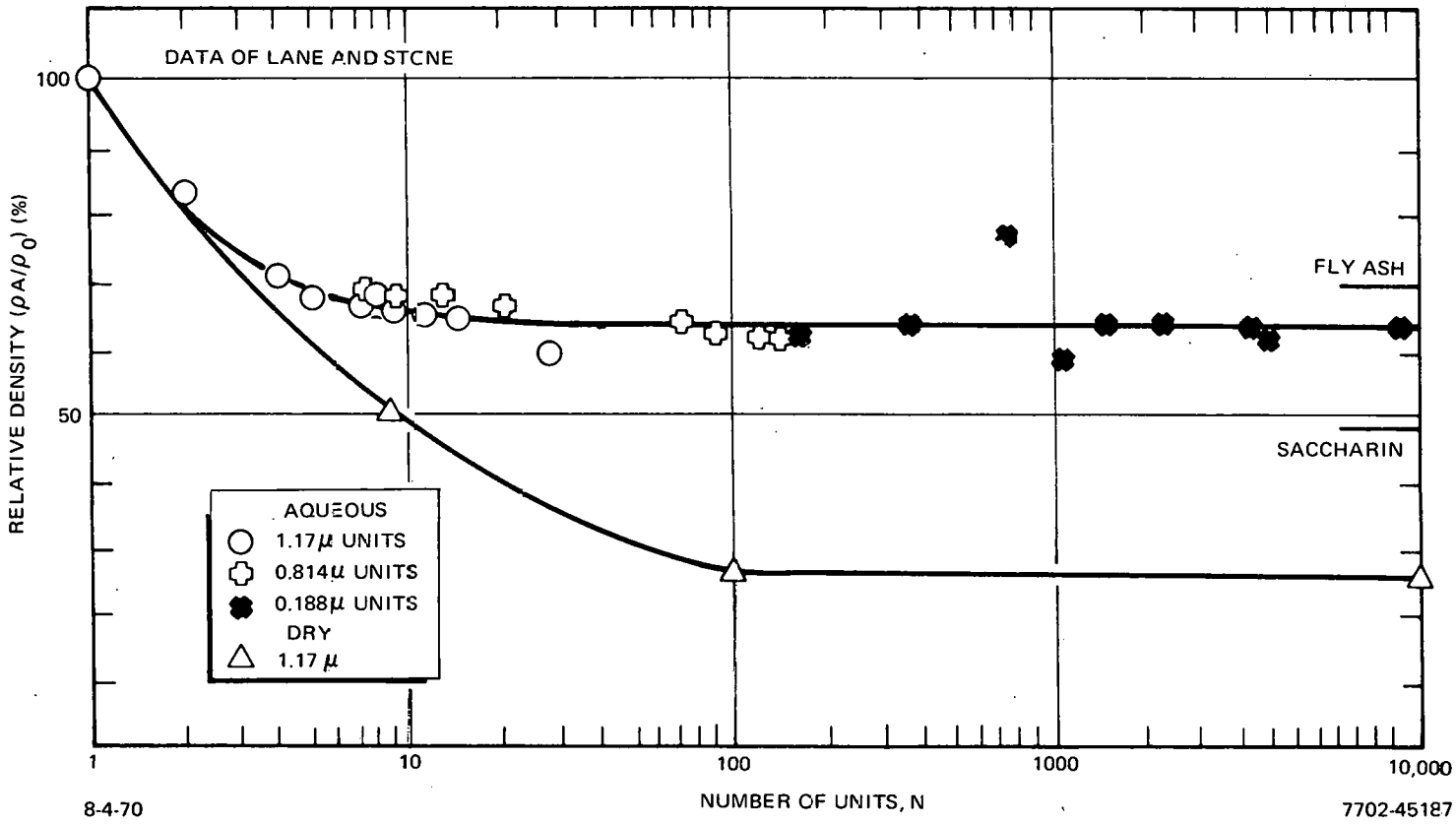

Figure 1. Variation of Density with Number of Particles in Aggregate Polystyrene Spheres Sprayed from Aqueous Suspension and Dry Powder

Recent work on the structure and density of agglomerates of both uniform and nonuniform spheres, with even larger numbers of particles in the agglomerate, has been reported by Lane and Stone.[35] They used the Millikan cell to measure settling velocity and particle mass. The studies were done with three basic sizes of polystyrene spheres (see Figure 1), a finely ground saccharin powder, and fine fly ash. Their studies of closed random packed agglomerates of polystyrene spheres sprayed from aqueous suspensions show that when the number of basic particles in the agglomerate is greater than ~10 the relative density is constant (see Figure 1). The results of Lane and Stone agree up to 11 particles with those of Stober. Lane reports that the agglomerates formed by spraying polystyrene spheres from an aqueous suspension have a limiting relative density of 0.63 independent of the basic size of the particles which form the agglomerate (0.2, 0.8, and 1.2 microns). Agglomerates formed from atomization of dry 1.2-micron polystyrene spheres, had a limiting relative density of 0.27 after about 100 particles had agglomerated. This was stated to be due to the formation of loosely packed nonspherical agglomerates. The limiting density for the fly ash was 0.69. This latter relatively insensitive change of density was postulated to be caused by aggregate formation of a basic 1-micron sphere coated with many finer particles. The saccharin powder was of intermediate packing density and had a limiting value of 0.49. No basic particle size was given for saccharin.

Earlier studies by Whytlaw-Gray and Patterson[29] of the density of agglomerates was limited to particles with radii between about 0.2 to 1.3 microns. Particles below 0.2 μ radius exhibited Brownian movement while particles above about 1.3 μ radius required such high potentials that ionization occurred in the Millikan cells used to measure settling velocity and mass of the agglomerated particles. While there was a trend to lower the smeared density as the agglomerate size was increased, enough scatter was present that the authors could only offer a statistical average for the materials studies. The apparent effect of particle size on the Stokes correction is similar to that reported by Lane and Stone when the number of agglomerates is less than 10.

Studies on the density of particle agglomerates were reported by Johnstone.[36] These studies were made for materials ranging in ideal density from 1.0 to 19 $\mu gm/cm^3$. Results very similar to those of Lane and Stone were reported.

Most of the agglomerates studied appeared to have already reached a constant density. Some materials, such as magnesium oxide, showed a dependence of density on size as reported earlier by Lane and Stone, and Whytlaw-Gray and Patterson. Johnstone's results for 0.33 and 1.17 μ-diameter polystyrene was much different from Lane and Stone, indicating that additional measurements are required.

It is difficult to separate the effects of agglomerate smeared density and shape factor on the settling velocity of a particle. Evidence confirming this problem is shown in the experimental data of Whytlaw-Gray and Patterson,[29] Johnstone,[36] and Lane and Stone.[35] Therefore, a Stoke's correction factor should be used to modify settling velocity calculations for agglomerated nonspherical particles as

$$V_s = \alpha V_I$$

where

V_s = settling velocity of agglomerate, with effective density and/or, nonspherical shape;

α = Stoke's correction factor = S.F.; and

V_I = settling velocity of equivalent sphere with ideal density.

The experimental data[35] on agglomerates of 1.17μ-polystyrene spheres indicate that the Stokes correction factor, α, decreases very rapidly with basic particle number to a constant value, $\alpha = 0.63$ for close randomly packed agglomerates (raspberries) of more than about 10 basic particles. The data also show that for nonspherical agglomerates produced by loose random packing of the same basic polystyrene particles, the limiting value of the Stokes correction factor, $\alpha = 0.27$, is obtained for agglomerates of more than $\sim$50 basic particles. Thus, the number of basic units of the agglomerates above which the correction to settling becomes constant varies with the tightness of packing. The equivalent or effective diameter of the agglomerate at which this occurs for loose random packing is $\sim$4 times the basic particle size.

2. The Effect of Particle Charges on Aerosol Coagulation

The coagulation constant of nonradioactive and radioactive metallic aerosols produced by an exploding wire technique has been determined experimentally by Rosinski, et al.[16] The temperature of the exploding wire was estimated to be 7000 to 8000°K. They found that in the early stage of agglomeration, the coagulation constant of radioactive gold aerosols (2 to 3.5 Ci/gm) was approximately 20 times the mean value of slightly radioactive aerosols (50 to 900 mCi/gm). They assume that coagulation is enhanced by the presence of highly ionized gas.

In a typical reactor site safety analysis, the initial radioactivity dispersed in the inner containment following the core disassembly DBA could be $\sim 2 \times 10^9$ Ci. If we assume that each disintegration produces one γ and one β particle of 1 Mev each, the initial production rate of ion pairs, q, can be about 10^{15} ion pairs/cm^3 sec (based on 32 ev/ion-pair and a volume of 1.5×10^5 ft^3). The recombination coefficient, a, is $\sim 2 \times 10^{-6}$ cm^3/sec per particle.[37] The rate at which the ion concentration varies, in the absence of particles is,

$$\frac{dn}{dt} = q - an^2 \qquad \ldots(18)$$

and at equilibrium, $q = a n^2$. Thus, the initial equilibrium concentration is $\sim 2 \times 10^{10}$ ion pairs/cm^3. The decrease in ion pair production rate (and hence the quasi-equilibrium concentration value) corresponds to the radioactive decay of the fission products.

The total released (initial) concentration is 200 μgm/cm^3, there are about 2×10^8 particles per cm^3. The agglomeration coefficient, K, is 3×10^{-10} cm^3/particles-sec and the rate at which the particles decrease in number by agglomeration is,

$$-\frac{dN}{dt} = KN^2 = 1 \times 10^6 \text{ particles/sec-cm}^3 . \qquad (19)$$

At the end of two minutes, the number of particles remaining unagglomerated is,

$$N = \frac{1}{Kt} = \frac{1}{3 \times 10^{-10}} \left(\frac{1}{2 \times 60}\right) = 3 \times 10^{7}$$

and after two hours, $N = 5 \times 10^{5}$. The table below compares the ion concentration with the particle concentration during the first two hours after the initial release (more than 90 percent of the total leakage to the outer containment occurs in the first two hours).

Time After Release	n (ion-pair/cm^3)	N (particles/cm^3)
0	2.2×10^{10}	2×10^{8}
2 min	1.4×10^{10}	3×10^{7}
2 hr	1.2×10^{10}	5×10^{5}

Of those particles which have agglomerated, their sizes have become large enough for them to settle. Thus, N decreases faster than n for two reasons: agglomeration and settling. There is always an excess of ion pairs over the number of particles.

If the N particles are positively or negatively charged, these particles would be in competition with the ions produced by ionization and would rapidly become neutral. One may therefore conclude that there will always be an excess of ion pairs, which, in turn, can only produce a bipolarly charged system of particles. As will be shown, such as system produces more rapid agglomeration than a neutral or unipolarly charged particle system. More rapid agglomeration would of course lead to increased particle size growth rates and hence higher settling rates and more rapid reduction of N.

Zebel[38] has shown that the agglomeration rate will depend on the degree of charging or specifically on the ratio of the number of elementary charges

(e) carried by the colliding particles, to the size of the particles. His formulation gives the ratio (z), of the agglomeration rate for a charged aerosol, to the rate for an aerosol under the influence of Brownian motion alone,

$$z = \frac{y}{e^{y} - 1} \qquad \ldots (20)$$

where

$$y = \frac{\frac{nme^2}{kT}}{r_n + r_m} \qquad \ldots (21)$$

$r_n + r_m$ = contact distance of the colliding particles,

kT = thermal energy, and

nm = numbers of elementary charges on each of the two particles. (n, m are positive or negative according to the type of charge involved; for the case under discussion, n and m are respectively positive and negative; therefore, the product must be negative. Thus for the present situation, y is a negative quantity.)

A sketch of this equation is shown in Figure 2. From this information, the agglomeration rate for a weakly charged bipolar aerosol, $y << 1$, is only slightly greater than that for an uncharged aerosol. For a strongly charged bipolar aerosol, y is a large negative number; in this case, agglomeration takes place at a much greater rate and settling of the particles will consequently be substantially accelerated.

Inasmuch as a reasonable postulation of circumstances which would lead to a monopolar aerosol has not been established, inhibition of agglomeration is not expected.

Experiments at Atomics International[24,39] and elsewhere have shown that chain-type agglomerates are produced during the vaporization of uranium oxide. Low concentration aerosol experiments at AI of uranium oxide and sodium

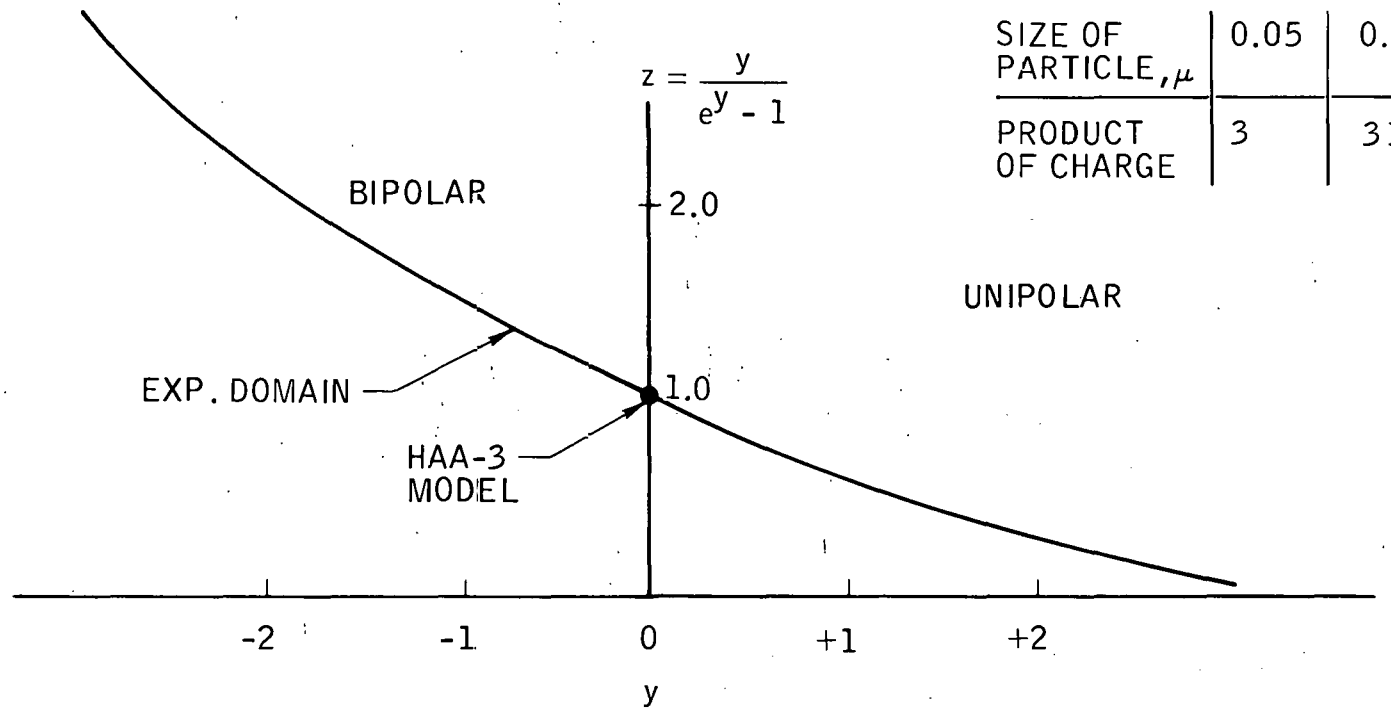

CHARGE – PRODUCT AT y = -1

SIZE OF PARTICLE, μ	0.05	0.5	5.0
PRODUCT OF CHARGE	3	31	310

70-A20-42-28

Figure 2. Charge Particle Effects

oxide mixture have produced a combination of spherical and chain-type aerosols. Therefore since chain-type particles are formed it is suspected that electrical coagulation has occurred and that sometime during the history of the aerosol bipolar charged particles existed. However, chain-type agglomerates can be formed from particle-dipoles. Such particle-dipoles usually occur during the heating of magnetic material particulates in the absence of oxygen.[29] Formation of chains of uranium oxide aerosol can be due to the later.

Experiments have shown that sodium oxide aerosols produced during a pool fire and spray fire have settled and plated according to the theory as previously discussed. Experimental data of plating rates on the test vessel wall have shown that unipolar charged particles are not formed, since such particles would repel one another and be attracted to the vessel wall independently of whether it was the floor or side walls.

3. Efficiency of Gravitational Collisions

If an aerosol particle falling with its terminal velocity overtakes a smaller particle falling with its smaller terminal velocity, it has been assumed that the particles will collide if they will be brought into contact by motion on straight vertical trajectories. This view over-simplifies reality, however, since it assumes that the air is stationary, whereas the impenetrability of the particles forces the air into motion that enables it to avoid the particles. If one particle had no size or mass, it would move with the air about it and so would not collide with the other particle. Collisions can only occur as corrections to this idealized view, as follows:

1) The particle has finite size. Hence, even though its center moves with the air and avoids the collision, its surface may extend far enough to encounter the other particle. This is the "interception effect."

2) The particle has greater inertia than the same volume of air. Hence its trajectory is straighter than the streamlines of the air, and so has a chance to encounter the other particle even though the streamlines do not. This is the "inertia effect."

See Figure 3 for a graphical demonstration of this effect.

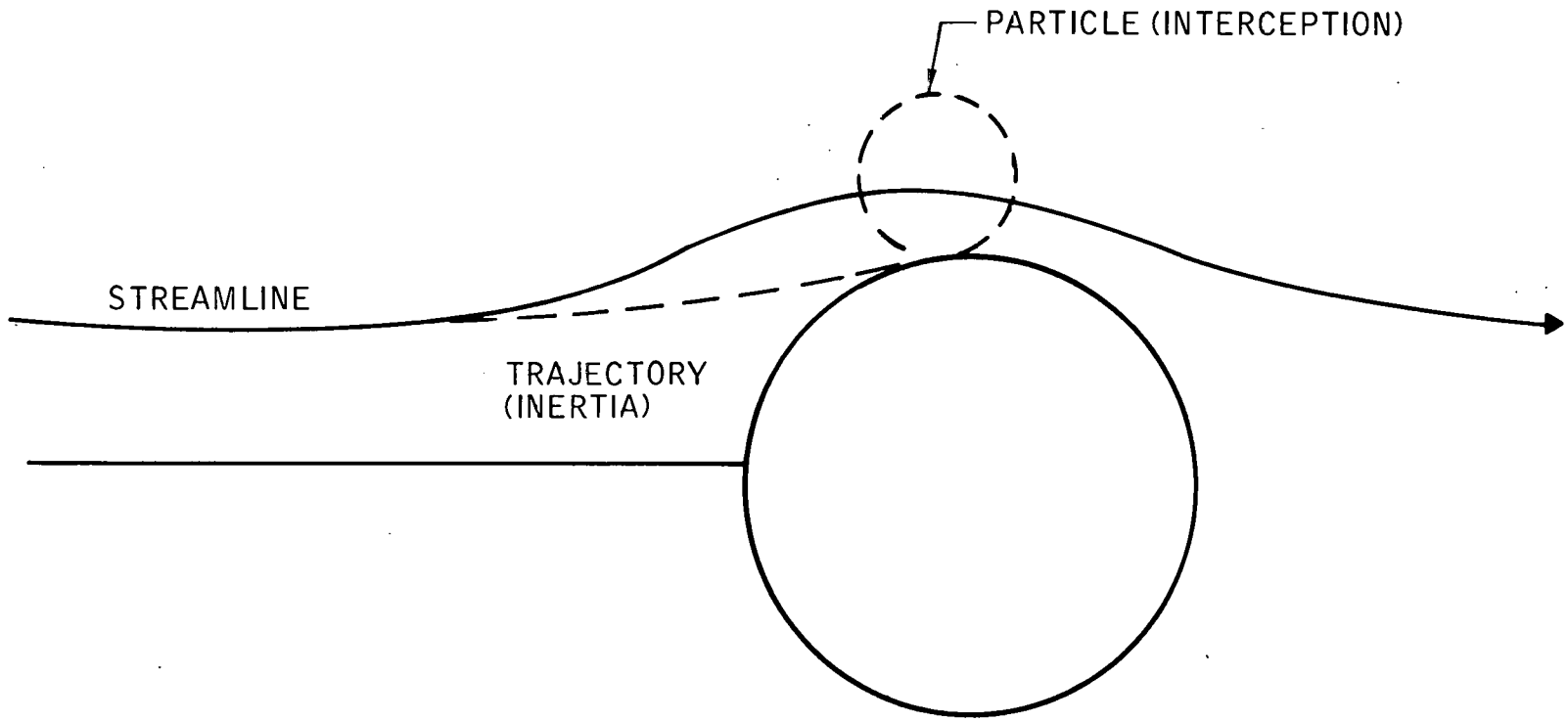

70-A21-42-51

Figure 3. Collision Mechanisms

There are theories of these two effects,[40] though they are limited to treating each effect by itself. Application to our problem indicates that the inertia effect is significant mainly for particles larger than we usually encounter. Attention will accordingly be confined to the interception effect.

The efficiency formula for interception-type collisions between spheres is commonly given[40] as

$$\mathfrak{z} = f(\kappa) \qquad \ldots (22)$$

where:

κ = ratio of small particle radius to large particle radius, r/R

$$f(\kappa) = \frac{\kappa^2 (3 + 2\kappa)}{2(1 + \kappa)} \qquad \ldots (23)$$

This is the factor by which the projected area of the larger particle must be multiplied to give the effective projected area for the collision (of Figure 4a). Since the assumption made hitherto in this report is that the trajectories are straight lines, we also require the corresponding factor for such trajectories, which is $(1 + \kappa)^2$. For our purposes, the efficiency is the ratio of these two factors:

$$\mathfrak{z} = F(\kappa)$$

$$F(\kappa) = \frac{f(\kappa)}{(1 + \kappa)^2} = \frac{\kappa^2 (3 + 2\kappa)}{2(1 + \kappa)^3} \qquad \ldots (24)$$

This is the factor by which the effective projected area for straight line trajectories must be multiplied to give the effective projected area for a motion in which the large particle moves on a straight line while the smaller one follows a streamline (see Figure 4a). This is not yet satisfactory, in view of the unsymmetrical treatment of the two particles. To improve it would constitute a major extension of currently available theories, however.

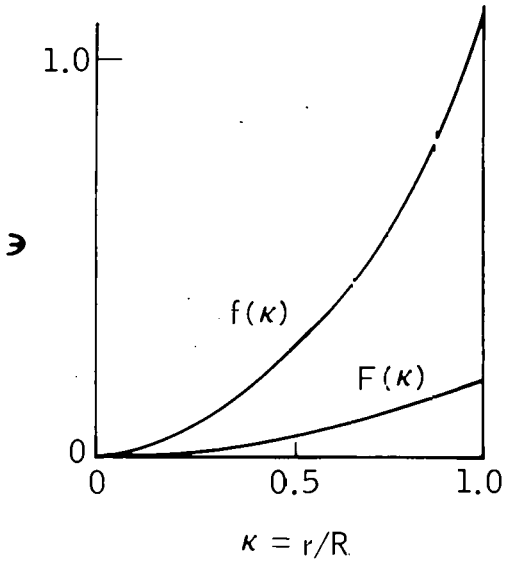

a. Efficiency of Interception vs κ

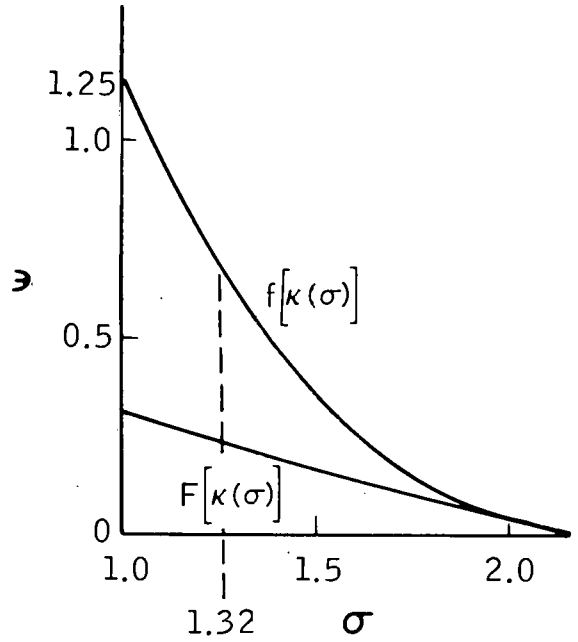

b. Efficiency of Interception vs σ

70-A21-42-52A

Figure 4. Particle Interception Effect

The effect of the efficiency factor $\mathfrak{z}$ on aerosol agglomeration is not immediately apparent from the preceding discussion, since a question remains as to which values of κ contribute to the process. This question has been treated by finding a representative value of κ for gravitational collisions according to the moments method and the log-normal approximation.[31] This is the value of κ at the maximum of the intergrand for the main term in the gravitational-agglomeration contribution to the rate-equation for the second moment (see Section IV-C).

The value is

$$\boldsymbol{\kappa}(\sigma) = \exp(-4 \ln^2 \sigma) \qquad \ldots (25)$$

where σ is the standard deviation of the distribution.

If this value is substituted for $\boldsymbol{\kappa}$ in Equations (23) and (24), representative estimates of the efficiency $\mathfrak{z}$ are obtained for the various values of σ (cf Figure 4b.) The significant range of σ is from about 1.3 to about 2, which is shown in Figure 5.

It is apparent that this theory of collision efficiency leads to a considerable reduction in the effectiveness of gravitational agglomeration, especially for the larger values of σ. Comparison of collision theory with experimental observations indicates that gravitational agglomeration is actually quite important in creating particles large enough to be removed rapidly by fallout (see Figure 6.) Furthermore, gravitational agglomeration with $\mathfrak{z} \gtrsim 1.0$ is necessary to explain the time behavior of r_v (see Figure 6).

One defect of the theory — its unsymmetrical treatment of the two colliding particles — has been noticed already. Another is the effect of Brownian motion, which acts qualitatively something like an increase of particle size. Thus Equation 24 becomes:

$$F(\kappa) = \frac{\kappa^2 (3 + 2\kappa)}{2 (1 + \kappa)^3} \cdot \zeta(r) \qquad \ldots (26)$$

where

$$\zeta(r) > 1 .$$

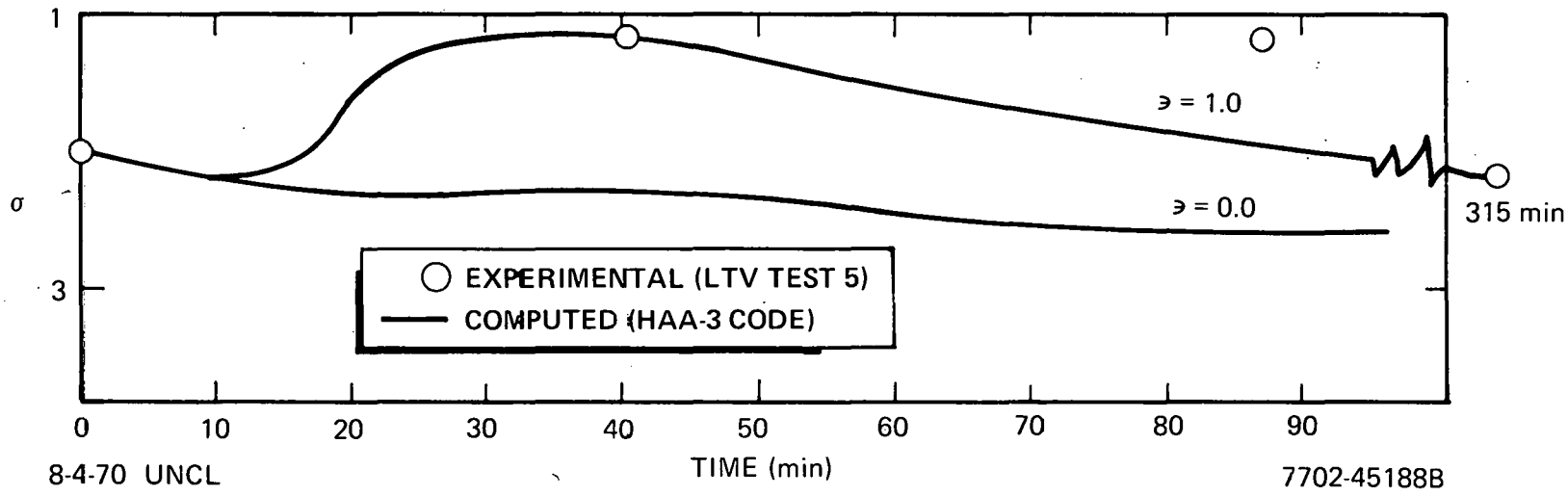

Figure 5. Particle Size Distribution Changes

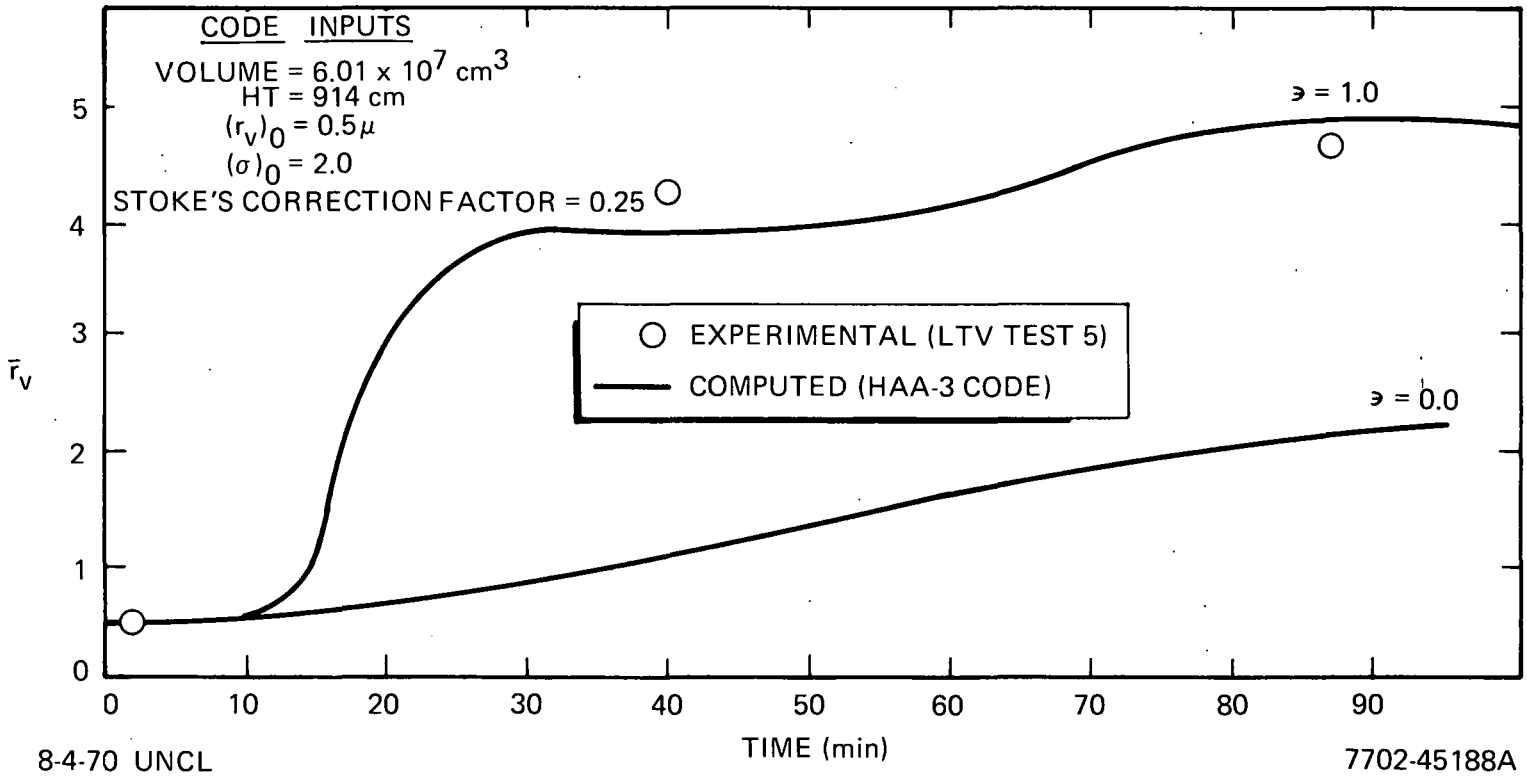

Figure 6. Effect of Collision Efficiency on Particle Size

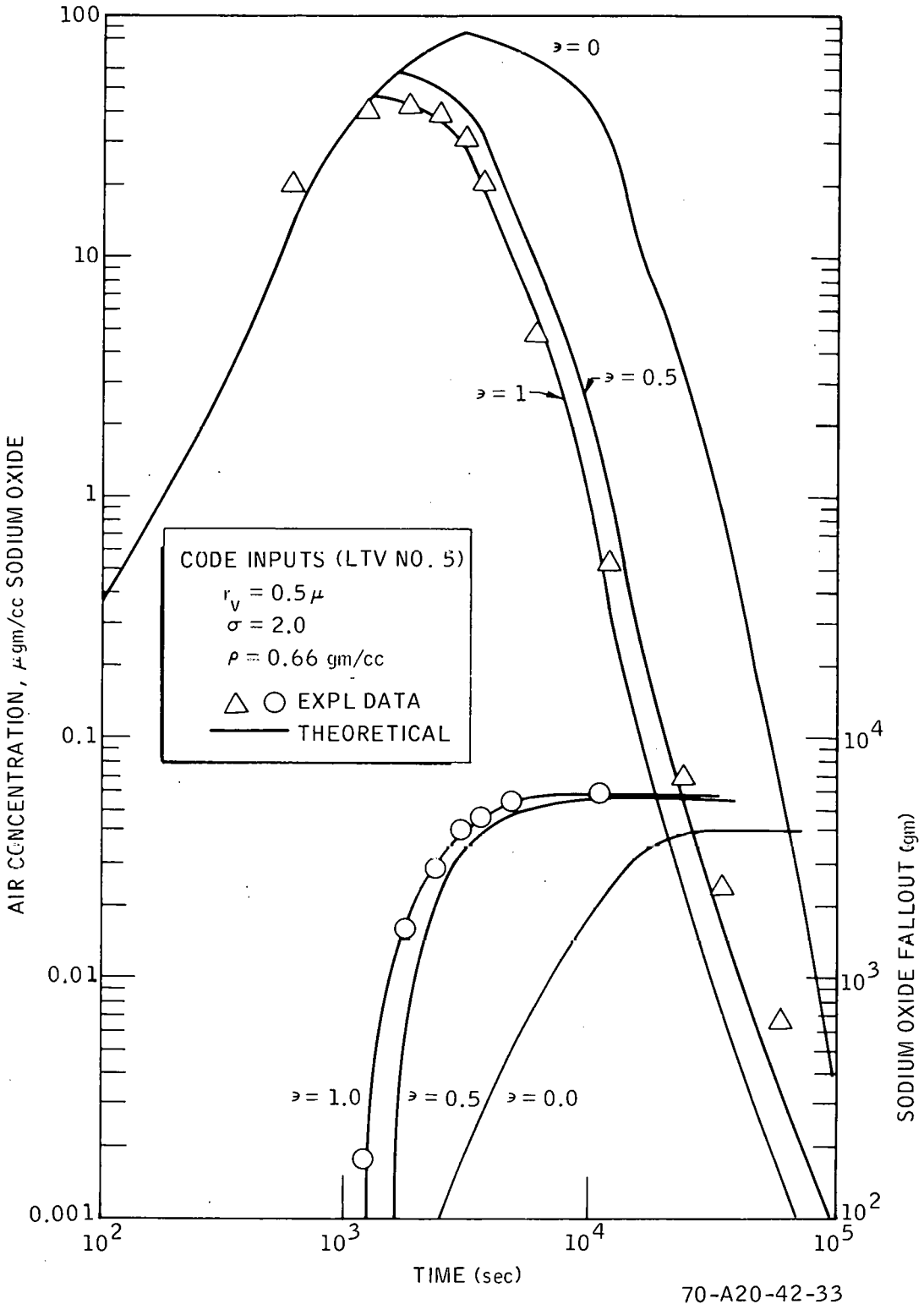

Figure 7. Effect of Collision Efficiency on Mass Transport Mechanisms (HAA-3 Code)

It is probable, however, that the principal defect of the Fuchs theory is the use of spherical particles. The actual shapes are often very far from spherical or any other simple regular shape. These irregularities modify not only the geometry of the collisions, but also the air motion near particles, which have been seen to be deeply involved in the collision process. Qualitatively, it is expected that the shape effect will be to increase the collision efficiency, since the deflections of the streamlines (and consequently of the trajectories) will tend to be controlled to a great extent by the small dimensions of the particles, whereas the probability of interception will tend to be controlled by the large dimensions. Irregularities will make the large dimensions larger and the small ones smaller, thus simultaneously reducing the deflections that prevent collisions, and increasing the range within which interception can occur. The effect of particle charge is also neglected in these theories. It is quite possible for these neglected effects to produce efficiencies approaching or exceeding unity. Consequently, there is no particular reason to suppose that collision calculations are made more realistic by reducing the efficiencies below unity, as required by the best current quantative theories, but refuted by the available experimental data on nonspherical aerosols. Needless to say, high concentrations, temperature gradients, particle shape, air movement all combine to increase the collision probability of particulates. Figure 7 shows the comparison of experimental air concentration and fallout data with HAA-3 code computations where gravitational efficiency is equal to one or zero.

It can be seen that the collision efficiency is ~ 1. This occurs because the study of the collision of spherical particles provides only a lower limit for the collision efficiency of agglomerated particles.

4. Turbulent Agglomeration

The two major mechanisms causing agglomeration, and included in the general integro-differential equation are Brownian diffusion and the effect of gravity. Turbulence is another mechanism for causing agglomeration, providing there is a sufficiently large dissipation rate of energy in the system.

Another important controlling factor is the sizes of particles involved. The following discussion will illustrate the numerical magnitude of these factors, and indicate the regime of importance for the various agglomeration mechanisms.

It has been shown that turbulence can cause collisions between neighboring particles in two ways:[11]

1) T_1 is due to spatial variations of the turbulent motion causing eddies to collide with one another, and thereby producing collisions between the particles entrained in the eddies;

2) T_2 is due to turbulent accelerations of an eddy and the size differences of entrained particles causing them to collide within an eddy.

Expressions for the rates of collisions for these effects have been shown to be:

Type	Rate
T_1	$n_1 n_2 \left(\frac{8\pi\epsilon}{15\upsilon}\right)^{1/2} (r + R)^3$ (ϵ = energy dissipation quantity)
T_2	$n_1 n_2 (8\pi)^{1/2} \left(1 - \frac{\delta'}{\delta}\right) \lvert(\tau_1 - \tau_2)\rvert \cdot \left[\frac{1.3^{3/2}}{\upsilon^{1/2}}\right]^{1/2} - (r + R)^2$ (υ is kinematic viscosity)

The relative importance of mechanisms for agglomeration may be judged by comparing the dependencies of the terms on the three parameters of consequence: the radii r and R, and the energy dissipation quantity, ϵ. The comparison is facilitated by considering radii with a fixed ratio $\kappa = \frac{r}{R} = \frac{1}{2}$. Smaller values of κ would correspond to lower number densities, and a comparison based then on r and ϵ would give some insight into the roles of these quantities.

With $\kappa = \frac{1}{2}$ the expressions for collision frequency (without the number density functions η_1, η_2; and with r and R in μ meters) become:

Brownian (B): $1.47 \times 10^{-10} \frac{(\kappa + 1)}{r}$

Gravitation (G): $8.44 \times 10^{-10} R^4 \left|\kappa^2 - 1\right| (\kappa + 1)^2$

Turbulence (T_1): $3.21 \times 10^{-12} \epsilon^{\frac{1}{2}} R^3(\kappa + 1)^3$

Turbulence (T_2): $2.46 \times 10^{-12} \epsilon^{3/4} R^4 \left|\kappa^2 - 1\right| (\kappa + 1)^2$

Note that the Brownian term does not depend on the radius R, providing the ratio κ is fixed. This is associated with the homogeneous form of the dependence on (r, R) for this term. It is helpful to take the ratio of each expression compared to the Brownian term, using $\kappa = 1/2$.

The relative terms are thus:

$$B = 1$$

$$G/B = 34.5\, r^4$$

$$T_1/B = 0.131 \epsilon^{\frac{1}{2}} r^3$$

$$T_2/B = 0.101 \epsilon^{3/4} r^4$$

This tabulation shows that the Brownian term will dominate for small radii. The ratio G/B = 1 for $r = 0.4\,\mu$, with Brownian strongly dominant for smaller values, because of the r^4 dependence. The tabulation also indicates that the turbulence terms will compete with the gravitational term only for high values of ϵ, the energy dissipation term. The ratio $\frac{T_2}{G} = 1$ for $\epsilon = 2400$. The dependence on r for both T_2 and G is the same, so that T_2 turbulence dominates for values of ϵ exceeding 2400 (ergs/gm sec = cm^2/sec^3). Since the dependence of T_1 on the radius is r^3, and the dependence on ϵ is as $\epsilon^{1/2}$, this term is always smaller than T_2. Its effect can be ignored, since it will always be less than some other dominating term. A sample tabulation of values is given, in Table III to illustrate the points made in this discussion.

Clearly the T_2 term for turbulence will be significant in causing agglomeration for large values of ϵ (>2500 cm^2/sec^3). If ϵ exceeds 10^3, the value is higher than any storm cloud turbulence which has been reported. Sedunov[41] has already concluded that turbulent acceleration does not contribute significantly to cloud particle growth.

TABLE III

RELATIVE IMPORTANCE OF TERMS ASSOCIATED WITH AGGLOMERATION MECHANISMS

Assume Ratio $\kappa = \frac{r}{R} = \frac{1}{2}$

All terms relative to Brownian Diffusion, (B)

Ratio → / ϵ →	G/B	T_2/B			T_1/B	
		10^2	10^3	10^5	10^3	10^5
r(μm)						
0.25	0.14	0.013	0.073	2.3	0.06	0.64
1.0	34.	3.2	18	5.6×10^2	4.1	41.
2.	5.5×10^2	5.1×10^1	2.9×10^2	9.0×10^3	33	330
4.	8.9×10^3	8.3×10^2	4.7×10^3	1.46×10^4	260	2600
8.	1.4×10^5	1.3×10^4	0.74×10^5	2.3×10^6	2.1×10^3	2.1×10^4
16.	2.3×10^6	2.1×10^5	1.2×10^6	3.8×10^7	1.7×10^4	1.7×10^5

In conclusion it can be stated that if intense turbulence does occur than it will aid in producing larger particles. The present model HAA-3A (see Section IV-C) omits turbulence and therefore may be conservative in the determination of particle size.

5. Resuspension of Deposited Material

Resuspension of deposited material in a closed cell would be evidenced by a persistent concentration of airborne material, the level of which would depend on atmospheric turbulence within the cell and adhesion forces of the deposited material, i.e., the air concentration in this cell would decrease only to a minimum level after some time in proportion to the source term. Resuspension has not been observed in the studies performed at Atomics International.[22-26]

Fine solid particles attach themselves indiscriminately to surfaces and to each other. The phenomenon is referred to as adherence and the strength of the bond is the force of adhesion. The efficiency of adherence of particles upon deposition on surfaces is still not resolved, and the re-entrainment of deposited particles has not been successfully analyzed. M. Corn states[42] that at present there is no satisfactory procedure for predicting the adhesive forces and re-entrainment factors from the physical and chemical nature of the particles and/or the substrate. However, experimental studies have been performed to measure adhesive forces and re-entrainment velocities for various particle systems.

The forces which contribute to the adhesion of particles are (1) London-Van der Waals dispersive forces, (2) electrostatic forces, and (3) surface tension of adsorbed surface films. All three forces have been studied so that some idea of their relative magnitudes have been obtained but even under the best conditions, the calculation of the adhesion forces of single particles is only an estimate.

Experimentally, it has been observed that a single particle will adhere to a surface with different strengths on repeated contact, due to the heterogeneity of the particle surface contact area. Small particle adhesion parameters are thus probable in nature and require statistical parameters for specification. This has led to the expression of experimental results in terms of the force required to remove a stated percent of a given size of adhering particles. Although

higher velocity air jets must be employed to dislodge particles from surfaces as particle size decreases, the force of adhesion decreases as particle size decreases.

The adhesive force is roughly proportional to the particle diameter and therefore smaller particles appear to adhere more tenaciously, even though the adhesive force between particle and surface is less than that holding a larger particle to the surface.

Most of the experimental studies to evaluate the resuspension factors have been performed with particles larger than 80 μm but some studies for smaller sizes have been made and the data can be represented by Table IV.

TABLE IV

RESUSPENSION FACTORS

Particle Size (μm)	Efficiency of Removal (%)	Air Velocity for Stated Removal (mph)	
		Mica	Glass
16	60	335	259
27	80	318	295
37	90	288	260

Engineering-type experiments have been performed to evaluate the resuspension of contamination from large areas due to natural and man-made forces.[43] In these empirical determinations, the resuspension factor, K, is defined as the ratio of the airborne concentration of the contamination due to resuspension, to the surface contamination per unit area:

$$K(m^{-1}) = \frac{\text{airborne concentration (units/m}^3)}{\text{contamination level (units/m}^2)}$$

Studies performed over soil surfaces uniformly contaminated with particulate uranium and polonium oxides have a mean value of K equal to 10^{-7} m^{-1} at wind speeds less than 10 mph.

In another series of tests, the resuspension factors for deposited zinc sulphide and copper oxide in a room 8 x 10 x 8 ft, were determined for various levels of activity within the room. The value of K was found to range between 10^{-7} and 7×10^{-6} m^{-1}, increasing as the degree of movement in the room was increased.

The resuspension factors for particulate plutonium oxide and plutonium nitrate on a laboratory floor were 10^{-7} m^{-1} for no movement in the room and 10^{-6} m^{-1} for vigorous movement within the room.

While there is no theoretical method presently available to evaluate the resuspension factors for deposited material, the experimental data from small-scale laboratory studies and from large-scale engineering type tests indicate that the contribution of resuspension of deposited material to the leaked mass following the DBA would be negligible and would not contribute to the environmental exposure.

C. HAA-3 CODE

An approximate solution of Equation 12 has been developed[31] by assuming that a log-normal distribution is maintained throughout the life of the aerosol. The integro-differential equation is replaced by three simultaneous, first-order differential equations in which the dependence on v has been removed. In order to do this, the form of the solution must be assumed. Since both experiment and previous calculations (Program HAA-2)[44] have indicated that the distribution of particles is very nearly log-normal, that type of distribution has been used. The formal expression for the log-normal distribution function is

$$n(v, t)\, dv = \frac{N(t)}{\sqrt{2\pi u(t)}} \exp\left[-\frac{\left[\ln \frac{v}{V(t)}\right]^2}{2u(t)}\right]\frac{dv}{v}, \qquad \ldots (14)$$

where:

$N(t)$ = total concentration of suspended particles (all sizes),

$V(t)$ = logarithmic mean volume of a particle times $3/4\ \pi$, and

$u(t)$ = logarithmic variance.

By using $\mu(t) = \ln V(t)$ and $S = \ln v$, the volume moments times $(3/4\pi)^k$,

$$X_k(t) = \int_0^\infty n(v, t) v^k dv,$$

may be evaluated; thus,

$$X_k(t) = N(t) \exp \left[k\,\mu(t) + \frac{1}{2}\, k^2 u(t) \right] \qquad \ldots (15)$$

In particular, the three moments are:

$$X_0(t) = N(t),$$

$$X_1(t) = N(t) \exp \left[\mu(t) + \frac{1}{2}\, u(t) \right],$$

and $$X_2(t) = N(t) \exp \left[2\mu(t) + 2u(t) \right].$$

In fact, the moment $X_0(t)$ is just the total number of particles, and hence identical with the parameters $N(t)$ already introduced. The moment $X_1(t)$ is just the total volume contained in the aerosol particles, and has the convenient property of being unaffected by coagulation. Both these moments, however, are relatively accessible to experimental determination. To give such quantities a central role is most appropriate. On the other hand, the higher moments are the ones most sensitive to the low-probability "tails" of the distribution, where the log-normal approximation is likely to be least satisfactory. In view of these considerations, the choice of moments is not really arbitrary. $X_2(t)$ is the distribution of the volume of the particles.

The HAA-3 program[45] can include in the moments equations any combination of settling due to gravity, wall plating, agglomeration due to Brownian motion, and/or agglomeration due to gravity.

The basic assumption in the approximate solution to the integro-differential equation for the behavior of an heterogeneous aerosol was that the aerosol distribution remained log-normal. This assumption is good as long as agglomeration is an important process. However, as the number concentration decreases with time, a point is reached at which the agglomeration

process becomes negligible. In the vicinity of this point the approximate solution becomes incorrect. If the behavior of the aerosol is to be calculated beyond this point, a more suitable approximation must be used.

To accommodate this problem, the approximate solution is used in the HAA-3 program until the ratio of the agglomeration rate to the settling rate reaches an input value, where the agglomeration rate is equal to or less than the settling rate. At this point the method of calculation is changed; a stirred settling model, SSM,[45] is used. In this model, the agglomeration processes are neglected. Only settling and leakage are considered, and the log-normal assumption is no longer required.

There is a separate SSM code available which can be used to calculate the size distributions of the airborne mass fraction and of the leaked mass fraction as well as the airborne mass, leaked mass, and settled mass fractions. This code, SMM-5,[46] computes particle size distributions by dividing the size range into 30 intervals and performing the Gaussian quadrature separately on each interval. The distributions calculated at selected times are printed and plotted at the completion of the calculations. If distributions are desired after the agglomeration rate is negligible, the SSM-5 code must be used instead of the SSM version in the HAA-3 program. This may be easily done by inputting into the SSM-5 code the log-normal distribution parameters calculated by HAA-3 at the time when the calculation switches to SSM.

An optional Klyachko velocity correction[45] is included in the HAA-3A program. This empirical correction includes the additional drag on a particle due to the inertia of air. It is important for combinations of larger particles and higher velocities, when the Reynolds number is greater than one.

A time dependent source rate is available as an option. The source rate function is input as a table of times and non-zero source rates. The function is linearly interpolated between input times. The source may be cut off at time τ. Alternatively a constant source rate or a no-source option may be used.

A time dependent leakage rate is also available as an option. The leakage rate function is input as a table of times and non-zero leakage rates. In the

HAA-3 calculations, the function is linearly interpolated between input times; but, in the SSM calculations, the function values R_i at time t_i is used over the interval t_i to t_{i+1}. Alternatively, a constant leakage rate or a no-leakage option may be used.

A modification factor, (Stokes factor) ALPHA, is available as an option. The settling rate of an aerosol particle is modified by multiplication of the ideal rate times ALPHA, which is assumed to be independent of particle size.

A constant efficiency, EFF, is a multiplier of all of the gravitational agglomeration terms in the moments equations. EFF must be set equal to 1.0 for 100 percent efficiency, and also is independent of particle size in the present model.

The total amounts per unit size that have plated, settled, and leaked at an output time are also calculated.

V. COMPARISON OF EXPERIMENT AND THEORY FOR THE COAGULATION OF AEROSOLS

A. CODE INPUT REQUIREMENTS

The purpose of this section of the report is to give the comparisons between experiments and the approximate solutions of the general equation programmed as HAA-3A. In such comparisons it is important to state clearly what assumptions are made, and to examine the parameters employed. Indeed if there are a sufficient number of parameter adjustments, the comparison becomes little more than curve fitting of the data.

A detailed derivation has been given of a general nonlinear integro-differential equation describing the behavior of a heterogeneous population of particles in Section IV-A. The equation is written in terms of the number density function for particles suspended in a closed vessel. The terms of the general equation include the effect of agglomeration and of various removal processes. The latter include removal by fallout, plating on walls, leakage (if such a pathway is present). There is also provision for a source term.

Numerical solutions of the general equation programmed as HAA-3A are compared to experiments performed in laboratories at Atomics International. The observations for which solutions are obtained are the:

1) Suspended mass concentration,

2) Mass of fall-out material,

3) Mass of wall plated material, and

4) Median size by volume of particle distribution.

These are obtained as a function of time.

As input for the integro-differential equation, one uses the observed initial distribution of the particle population (initial) median size by volume, $r_v(o) = 0.5$, and geometric standard deviation, σ, equal to 2, based on the assumption of an initial log-normal distribution. One also uses as input the observed released mass, M_R, or its counterpart the observed released mass concentration, $C_R = M_R/V$. M_R is the total mass released and is distributed

at any moment as suspended material, fallout or plated material. The quantity V is the volume of the chamber into which the particles are released.

The constants appearing in the general equation are either known physical constants or are constants describing the geometry of the container. The only "undefined" parameter is a wall plating constant whose value is estimated by an actual measurement. The plating constant was discussed in Section IV-A.

One of the physical constants is the material density, which is used in the expression giving the fall-out velocity in the Stokes-Cunningham expression. It has been shown in Section IV-B-1 that agglomerated particles tend to form voids, even when close packing occurs, which reduces the effective density (Stokes velocity) to a fraction of the unit particle density. The relative density is a function of the number of particles that have agglomerated, reaching a stable value which is constant no matter how large the agglomerated particle may be. For spherical particles agglomerating to form nearly spherical clusters, an effective density of about 63% of the unit density is reached when the agglomerated particle is about 3 times as large or larger than the unit particle size. (The new effective diameter is 3 times larger). For particles that join to form agglomerates that are not closely approximated as spherical clusters, the packing is looser with greater percentage of voids. In one such case,[36] the agglomerated particles reached a stable percentage of approximately 25% of the unit particle density when the effective diameter was about 5 times the unit particle size of 1.17 μm. Smaller unit sizes will proportionately result in smaller stable relative diameters. This smaller agglomerate diameter requires a larger particle population to produce the same size aerosol that a few particles would produce. On the basis of this work we have assumed that if the mean size exceeds 5 times the original unit size, then the loosely packed effective density of 25% is used in the Stokes expression. It will be shown that this simple assumption allows agreement between experiment and computation for the AI data obtained at high concentrations in a large test vessel.

The experimental-model comparisons which are the basis for reactor safety applications used values of α between 0.25 and 0.5 for code inputs to estimate the behavior of aerosols at high concentrations in large vessels. For the fuel and sodium agglomerates of interest in reactor safety, the absolute value of the density which has been used is 1 gm/cm^3. The value of α is dependent upon the density of the mixture of fuel, sodium and fission products which is released at the time of the hypothetical accident. The estimated ideal densities of the mixture varies from 3 to 6 gm/cm^3 and the Stokes factor α varies from 1/3 to 1/2 very similar to those used in the correlation of experiment and theory in the following section.

B. COMPARISONS WITH EXPERIMENTS IN LABORATORY TEST CHAMBER (LTC)

Reference 44 gives a detailed account of the comparison for experiments in which the mass concentration released, C_R, was of the order of a few (up to 4) $\mu gm/cc$. The report shows quite good agreement with the observed mass concentration of suspended material, mean radius by volume, and settled and plated masses, all as a function of time. What is noteworthy is (a) the simultaneous fitting of theory to 4 sets of data, and (b) there are no adjustable constants and only one adjustable parameter (wall plating distance) (see Section IV-A.)

The LTC chamber is 6 ft high and has a volume of 40 ft^3. In metric units: h = 180 cm; $V = 1.13 \times 10^6$ cm^3.

The restriction of comparison of theory and experiment to 4 $\mu gm/cc$ for C_R is due to a limitation of the HAA-2 computer code originally used to solve the general equation. This restriction was in effect removed by creating the HAA-3 computer code which uses an alternative method, the moments methods, to solve the general equation. This method[31] is described in Section IV-C in this report. Comparison calculations made using the moments method (Program HAA-3) and the earlier numerical method computer solution (Program HAA-2) yielded almost identical results (to within a few percent). The moment method of solution was used for the experiments described below.

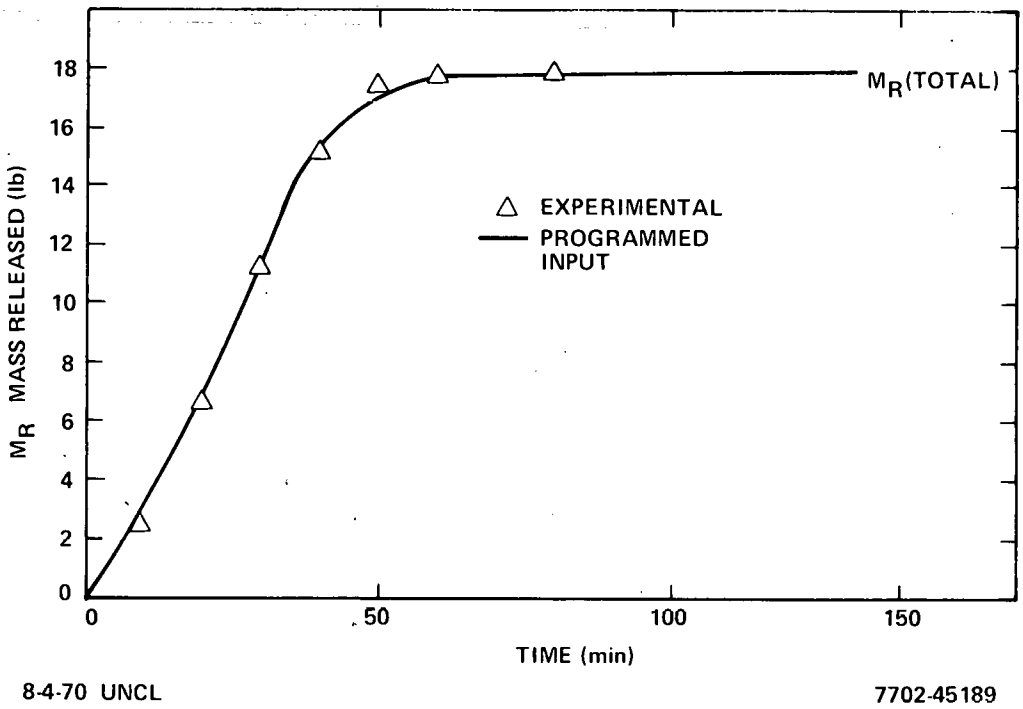

Figure 8. Mass Release Rate for Test No. 3

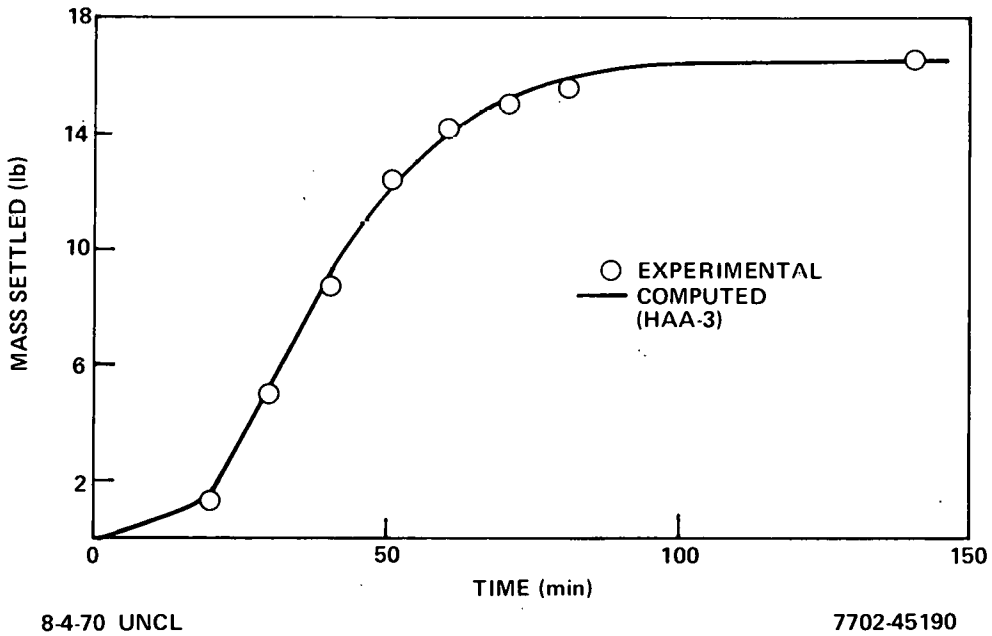

Figure 9. Settled Mass for Test No. 3

C. COMPARISONS WITH EXPERIMENTS IN THE LARGE TEST VESSEL (LTV)

1. General

The LTV is 900 cm in height, h, and has a volume, V, of 6.0×10^7 cm^3. Thus this vessel is larger in volume than the LTC by a factor exceeding 50. Sodium burning experiments were performed with released mass concentrations as high as 175 μgm/cc as oxide (about 130 μgm/cc as sodium). The observed increases in median radius by volume were of the order of 4 to 5 μm, some 8 to 10 times as large as the measured initial size of 1/2 μm. For such cases an effective density of 25% of the ideal is assumed, based on the discussion given previously. Actually we have employed the term Stokes factor (α) to be used as a multiplier in the traditional expression for the Stokes velocity. Thus, α includes both effective density and possible effect of shape.

2. Discussion of Test 3

Figure 8 is a graph of the observed released mass that was used as the input for the computer solution. Figure 9 is a graph showing the comparison between experimental data and the computer solution for the settled mass. The agreement is good. Figure 10 is a graph of observed mass concentration of suspended material and of the corresponding computer solution. Agreement is reasonably good. Figure 11 compares data with computer solution of the suspended mass concentration for later times. Agreement is reasonably good for several decades of values of C. Figure 12 is a graph comparing observation with computer solution for the median radius by volume. It is noteworthy that both the observed data and the computer solution indicate very large values up to 5 to 7 μm. The maximum computed size exceeds the maximum observed by some 27%. The values observed and computed for later times agree to within 10%.

It may be concluded that the 3 sets of data of Test 3 are well represented by the theoretical calculations.

3. Tests 4 and 5

Figures 13 through 17 show the same kind of comparison for Test 4; similarly Figures 18 through 22 correspond to Test 5.

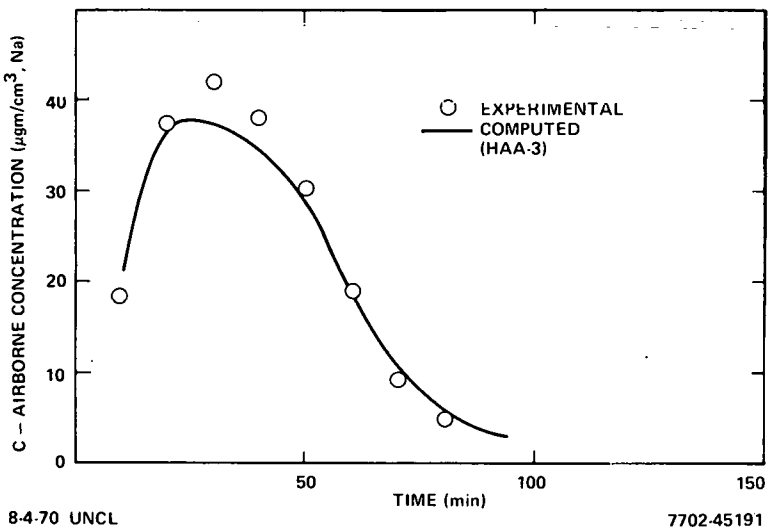

Figure 10. Airborne Mass Concentration for Test No. 3

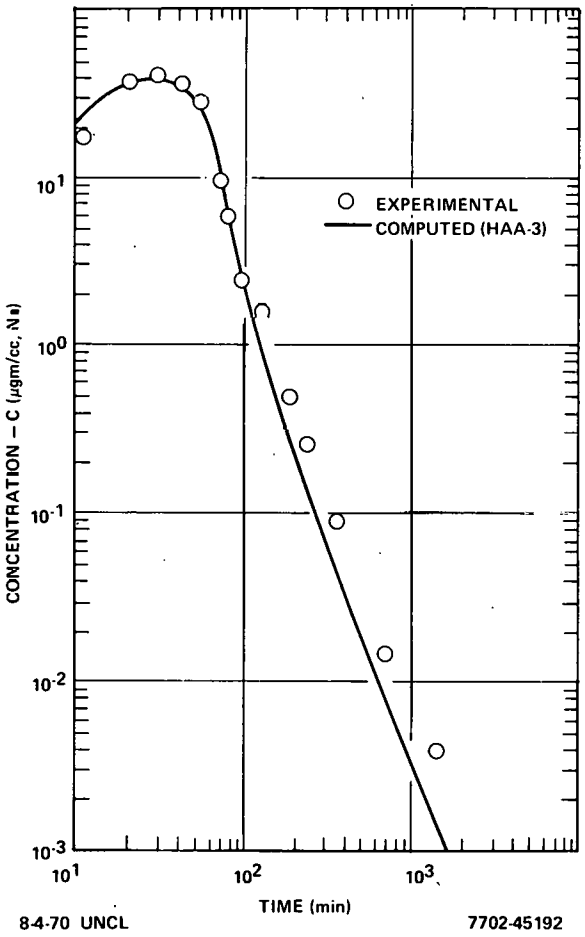

Figure 11. Airborne Mass Concentration at Extended Time for Test No. 3

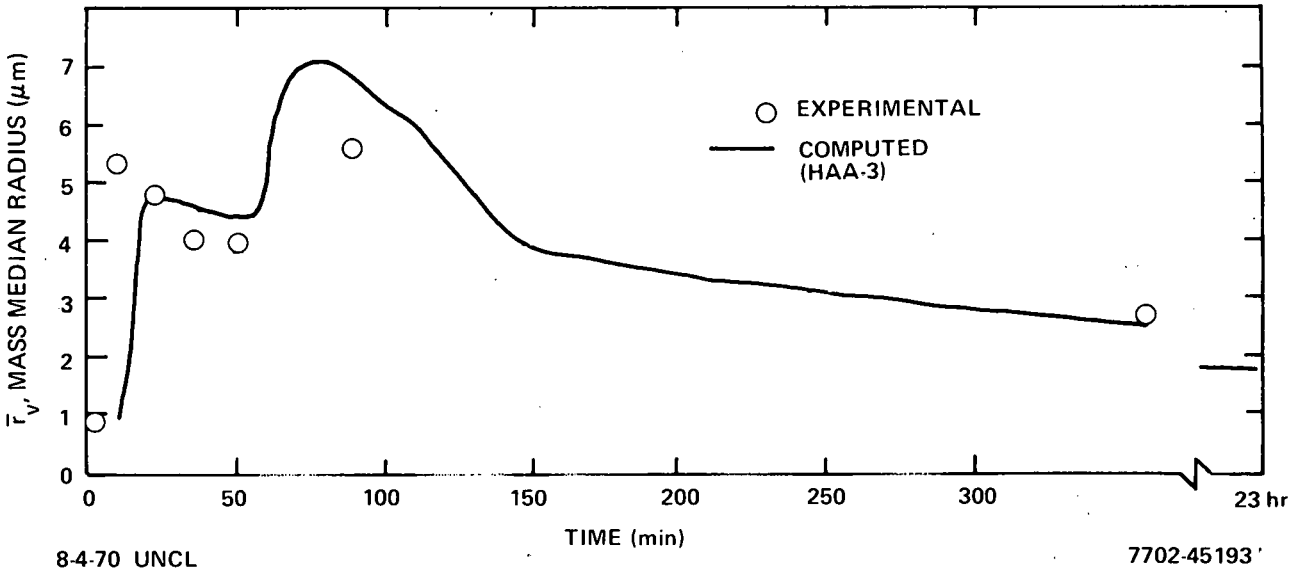

Figure 12. Median Airborne Particle Size for Test No. 3

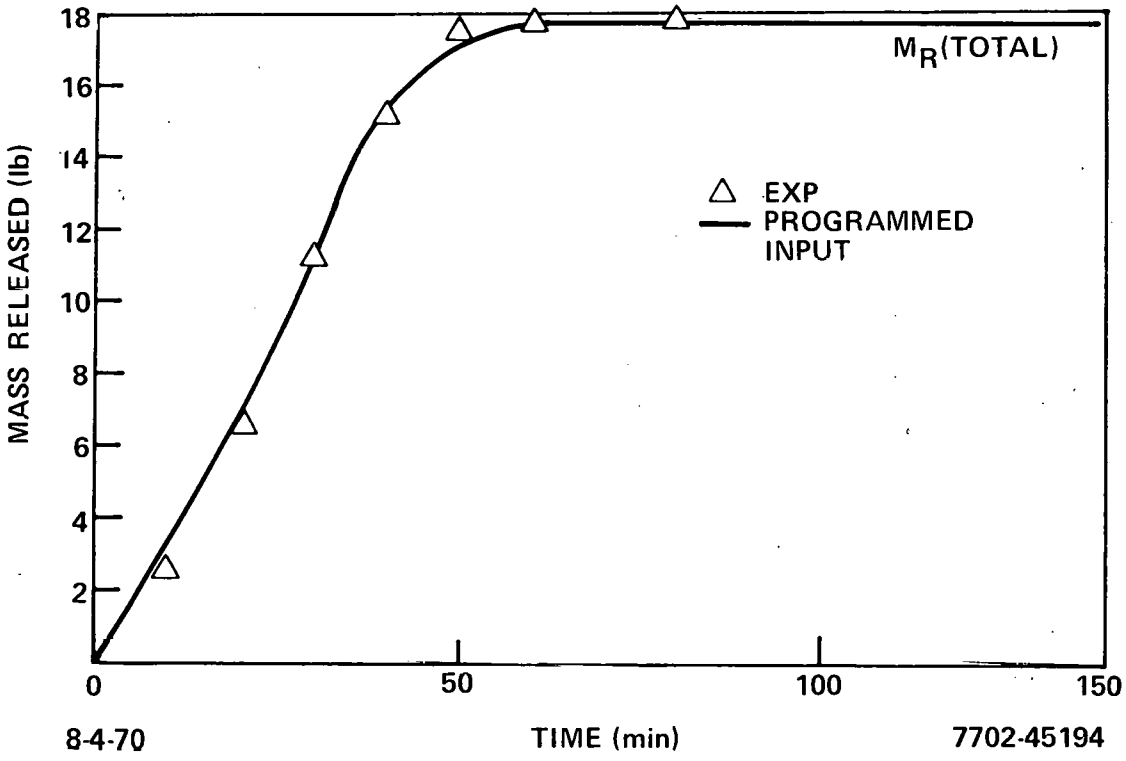

Figure 13. Mass Release Rate for Test No. 4

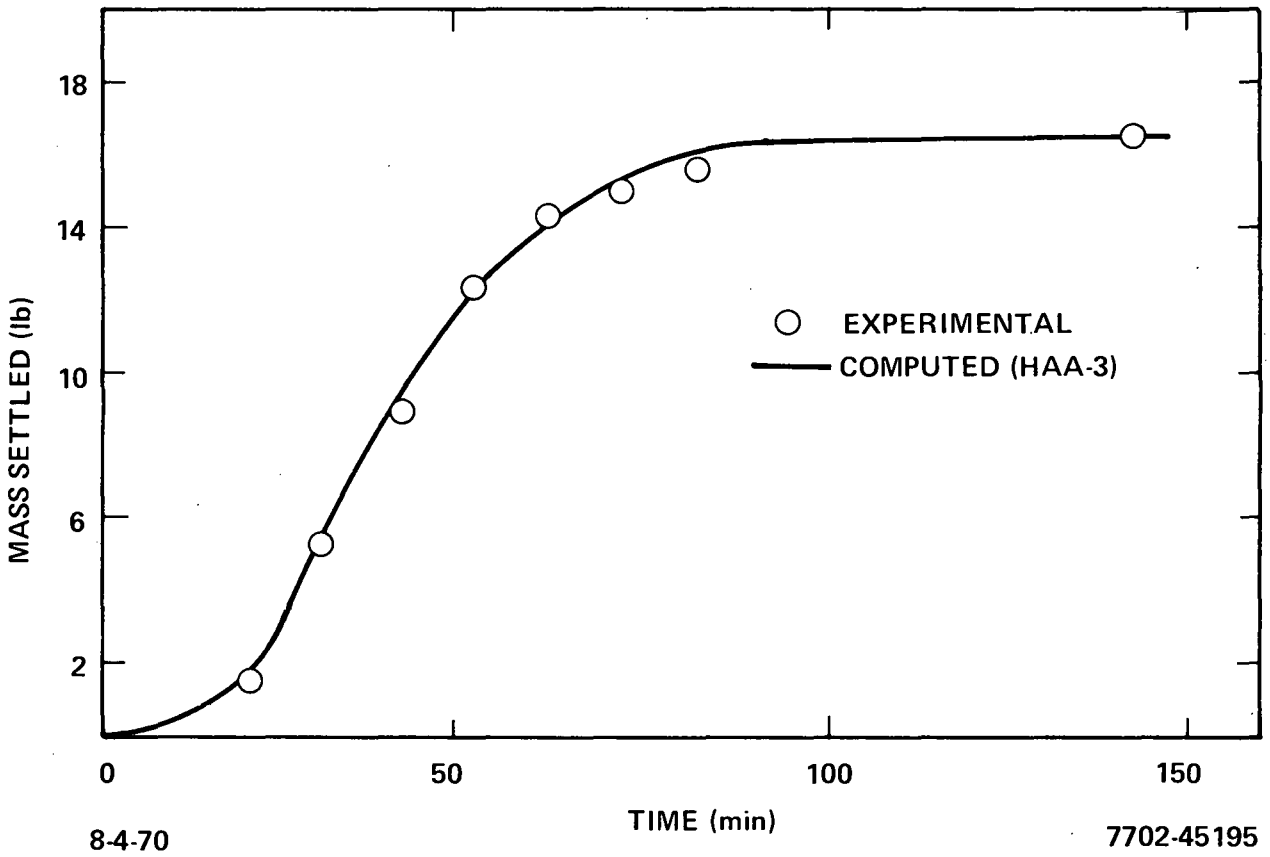

Figure 14. Mass Settled for Test No. 4

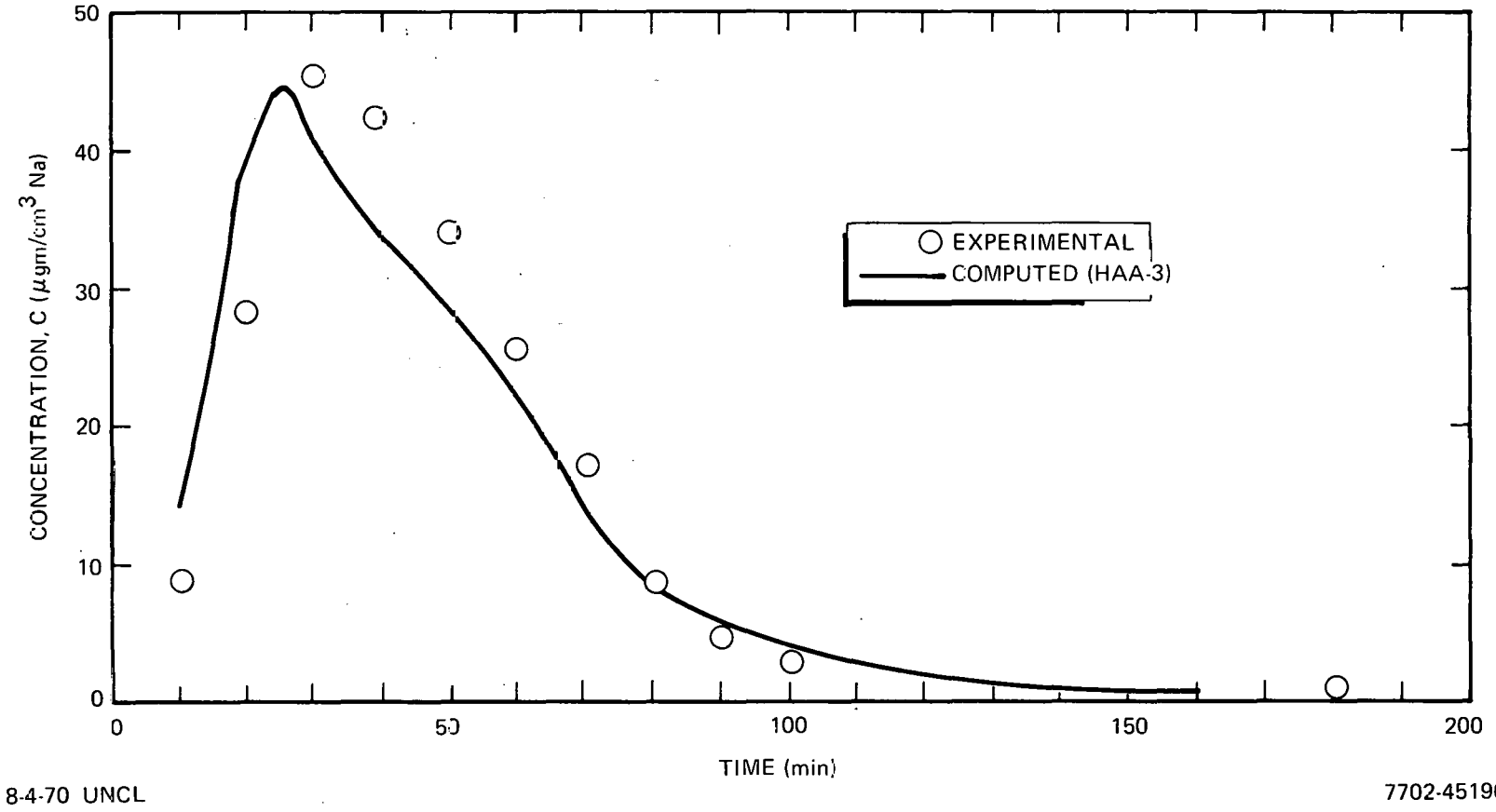

Figure 15. Airborne Mass Concentration for Test No. 4

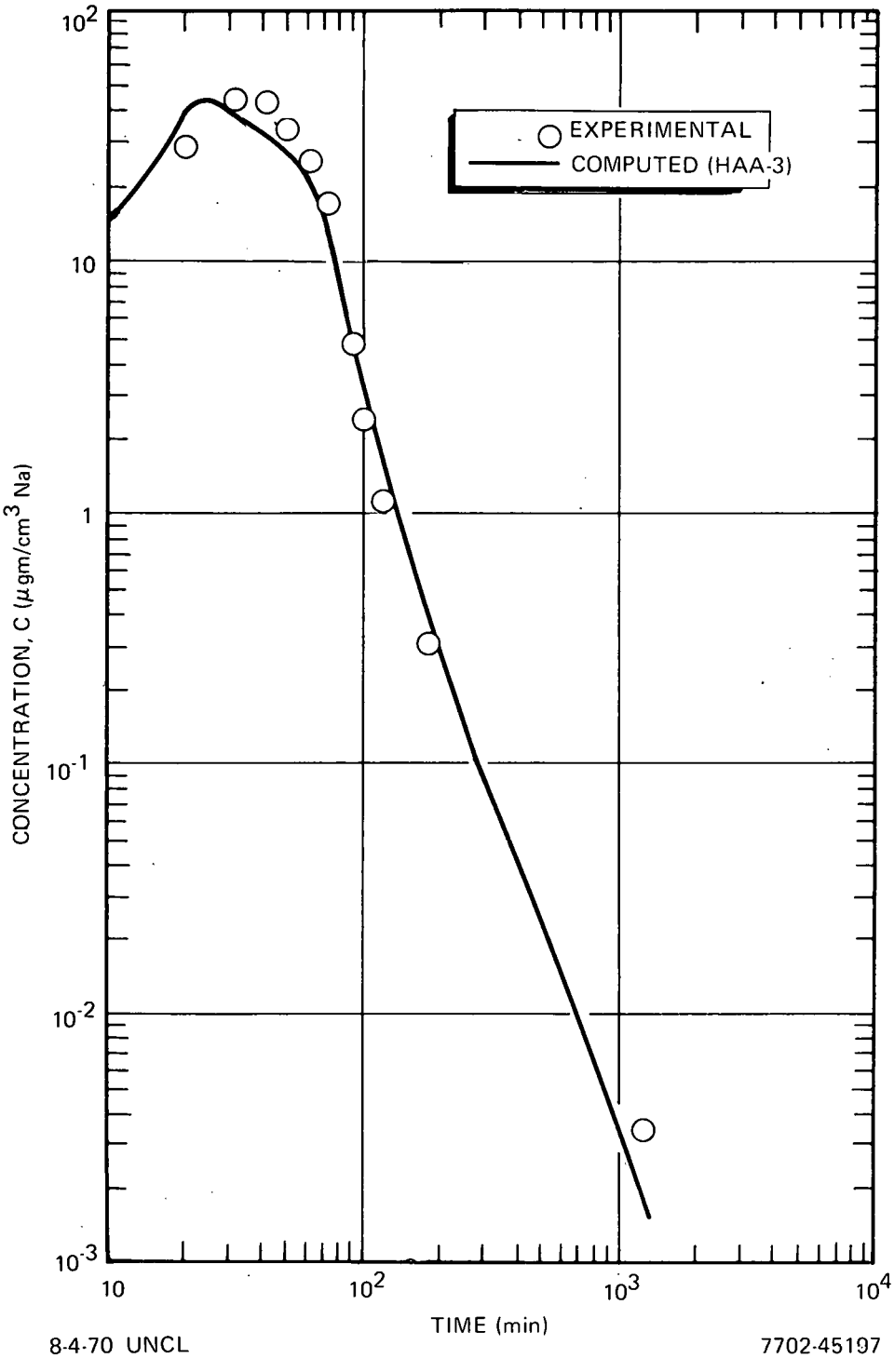

Figure 16. Airborne Mass Concentration at Extended Time for Test No. 4

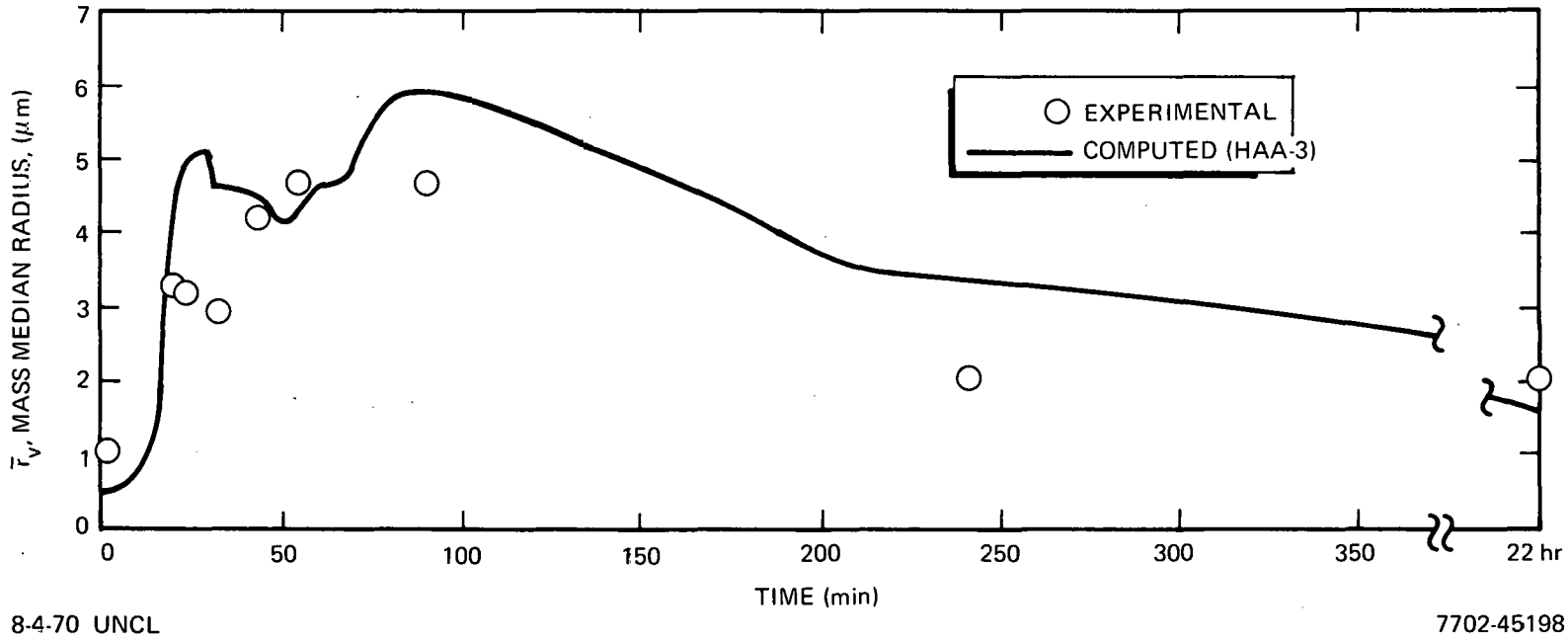

Figure 17. Median Airborne Particle Size for Test No. 4

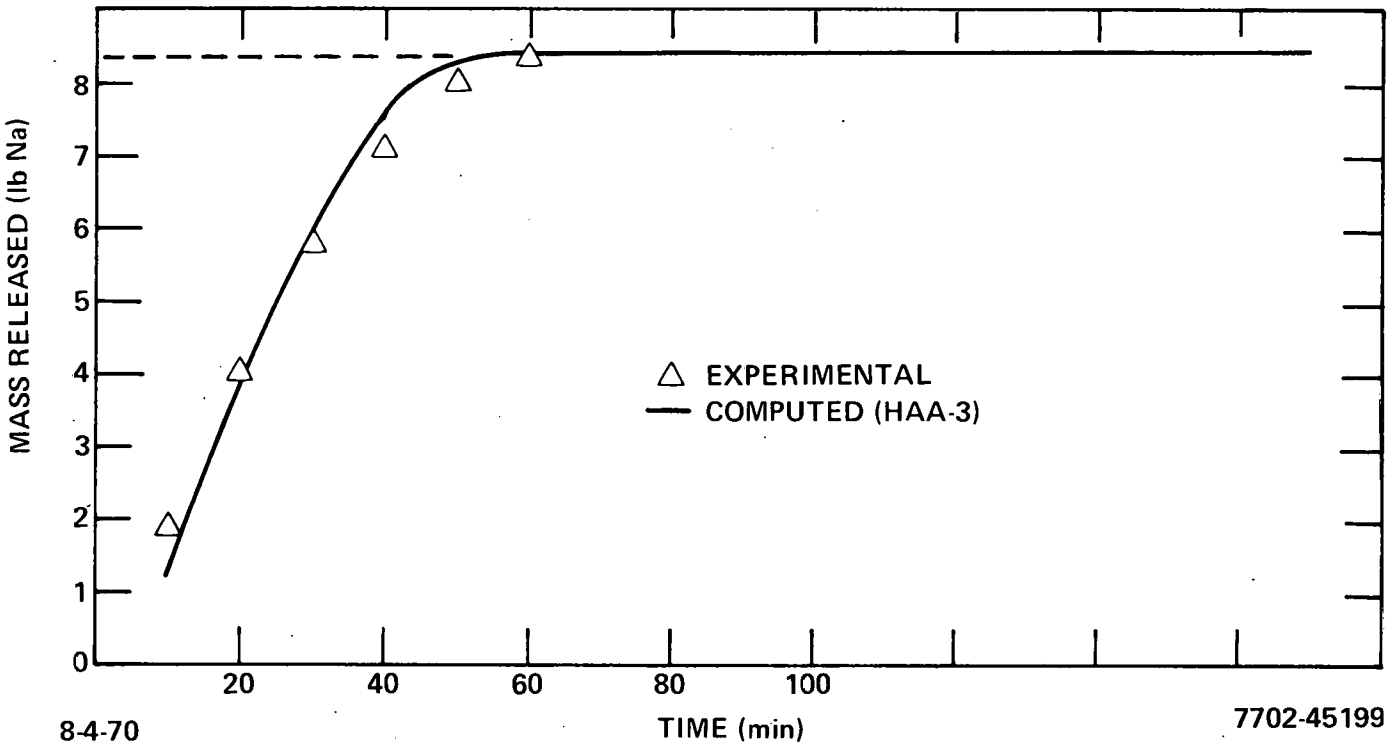

Figure 18. Mass Release Rate for Test No. 5

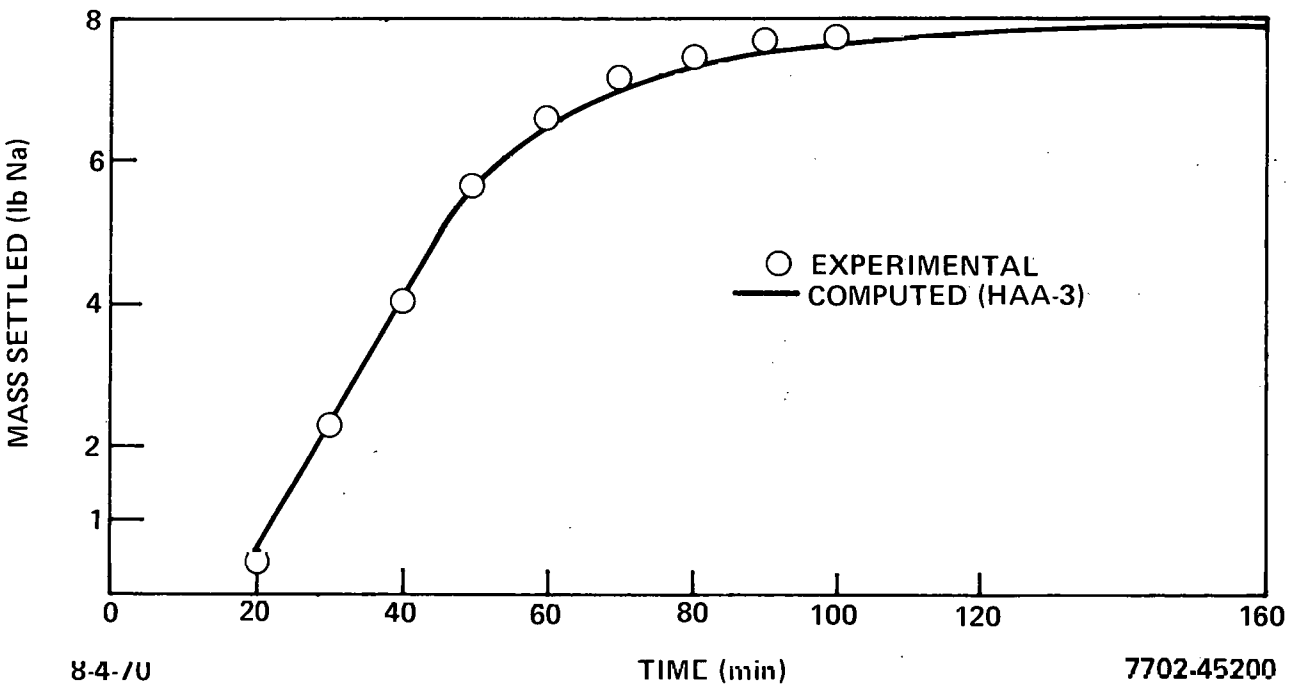

Figure 19. Mass Settled for Test No. 5

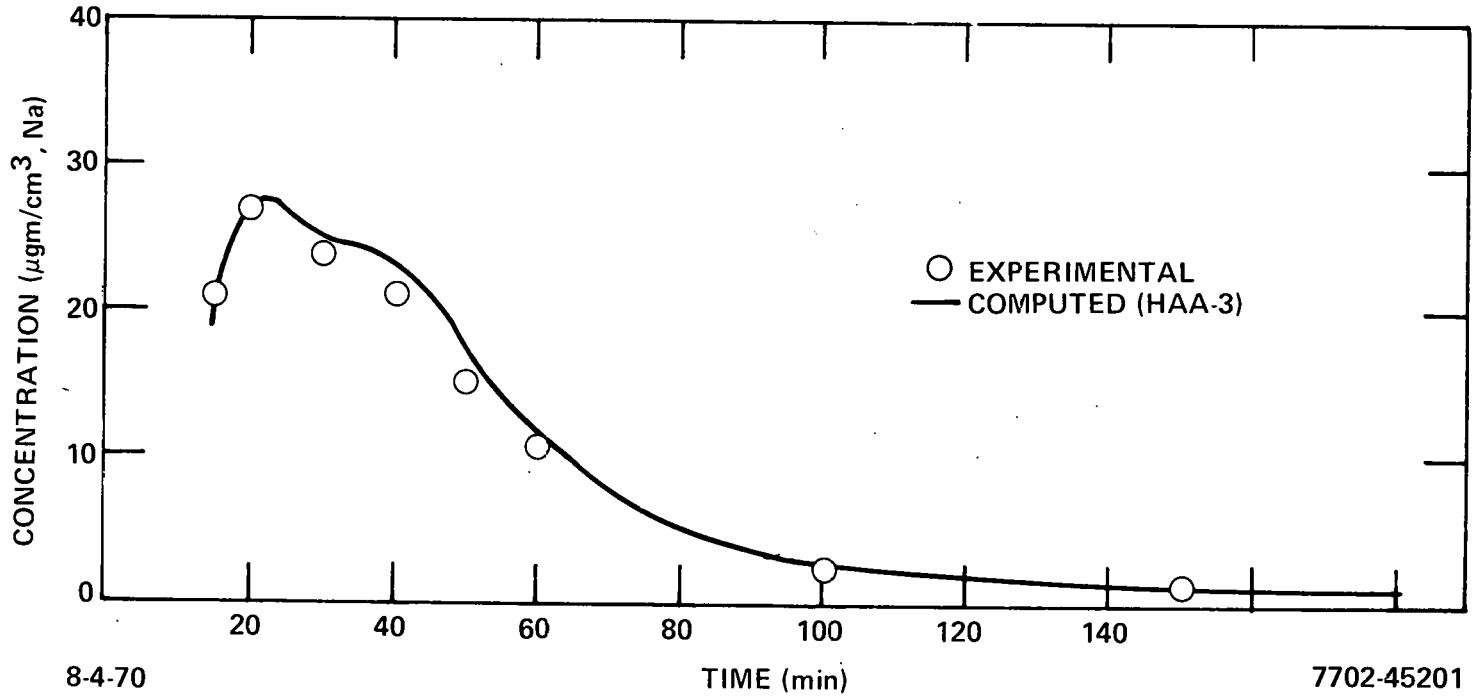

Figure 20. Airborne Mass Concentration for Test No. 5

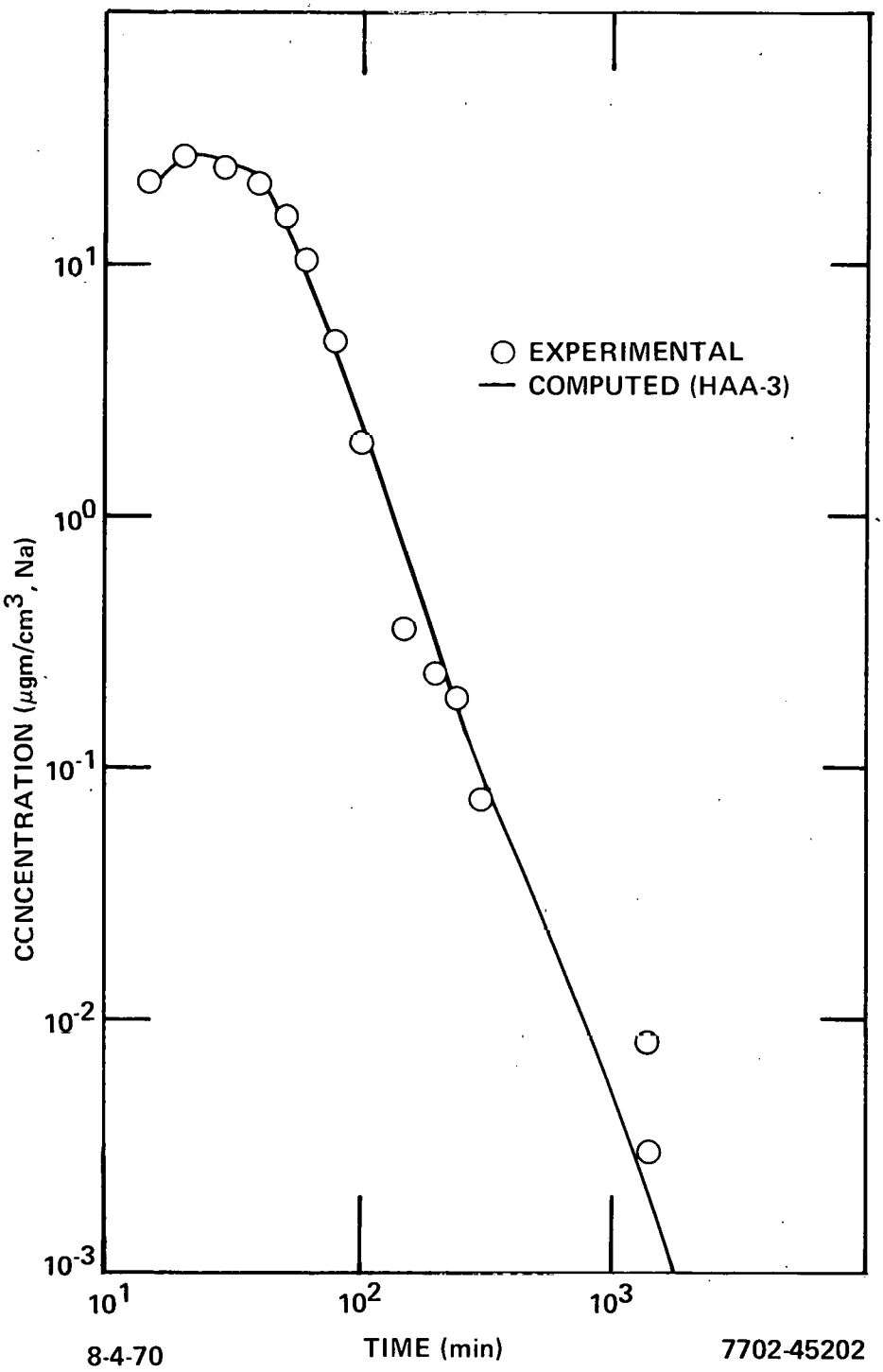

Figure 21. Airborne Mass Concentration at Extended Time for Test No. 5

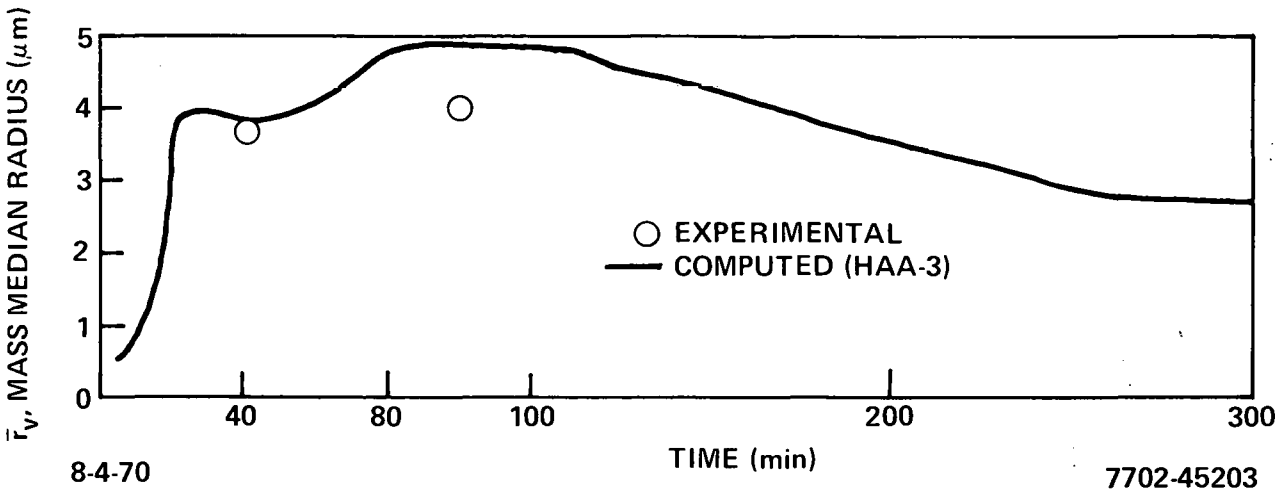

Figure 22. Airborne Particle Size for Test No. 5

It is clear that the nature of agreement for the same 3 sets of parameters between theory and experiment for Tests 4 and 5 are as good as these described for Test 3.

4. Test 6

In this case the released mass concentration is relatively low (<1 μgm/cc) and the observed growth in median size by volume in modest (less than a factor of two). Nevertheless the computer solution follows the data fairly well. Figures 23 through 27 show that the agreement is still good.

Table V lists the input parameters, based on observation, for Tests 3, 4, 5, and 6. Tests 3, 4, and 5 involved relatively large released masses of approximately 8000 and 4000 gm of sodium. The corresponding values of the released material concentration is of the order of 130 and 65 μgm/cc (as Na), larger than the maximum studied in LTC by a factor exceeding 2. The initial oxygen concentration was 21% for Tests 3 and 4, and 9.25% for Test 5. Test 6 is quite different from the other in a number of important ways: (1) initial oxygen concentration was 2%; the value of M_R = 36 gm (Na), with C_R = 0.6 μgm/cc (Na), quite low compared to the others. The shape factor for Test 6 is 1.0 since maximum particle growth did not exceed the original size by 5.

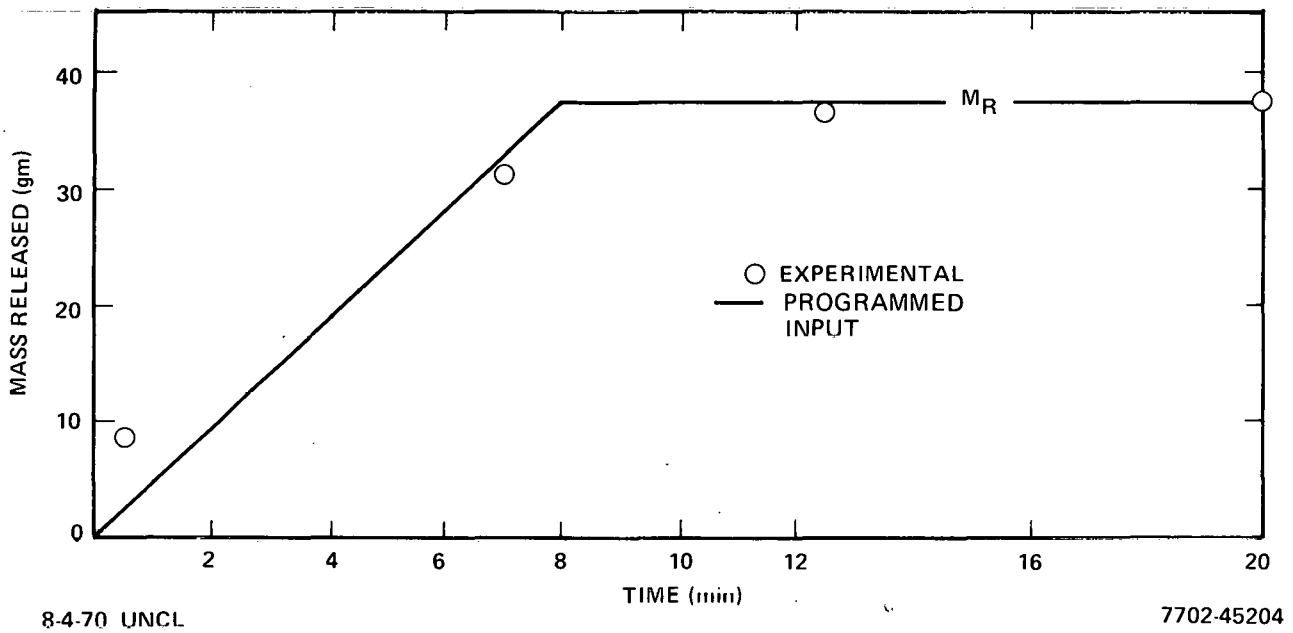

Figure 23. Release Rate for Test No. 6

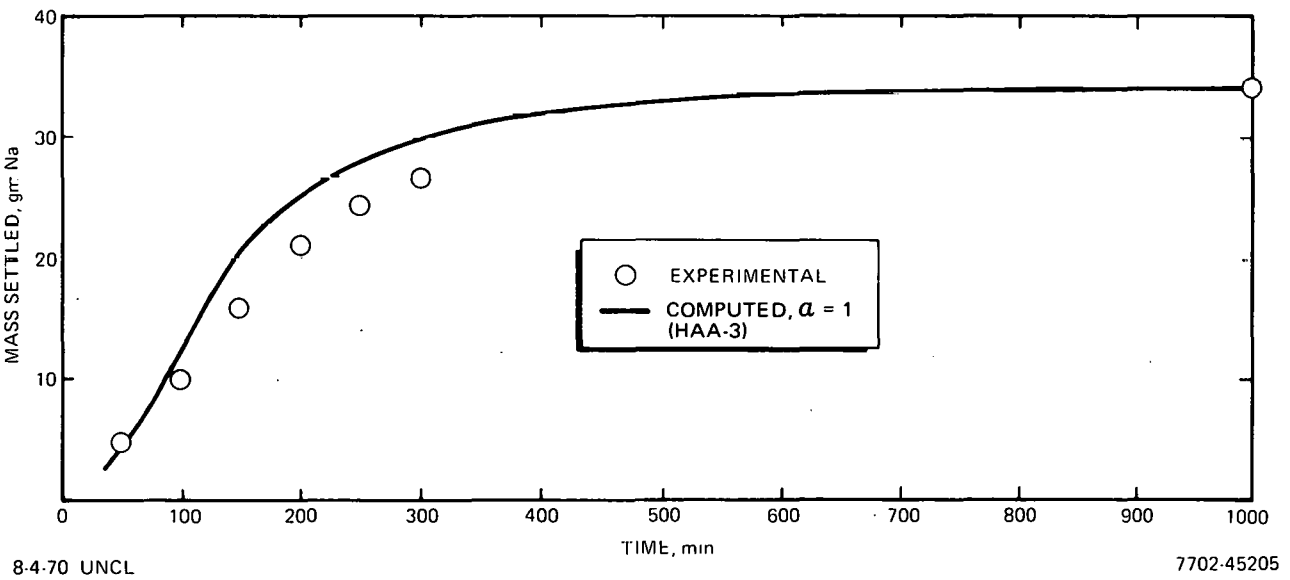

Figure 24. Mass Settled for Test No. 6

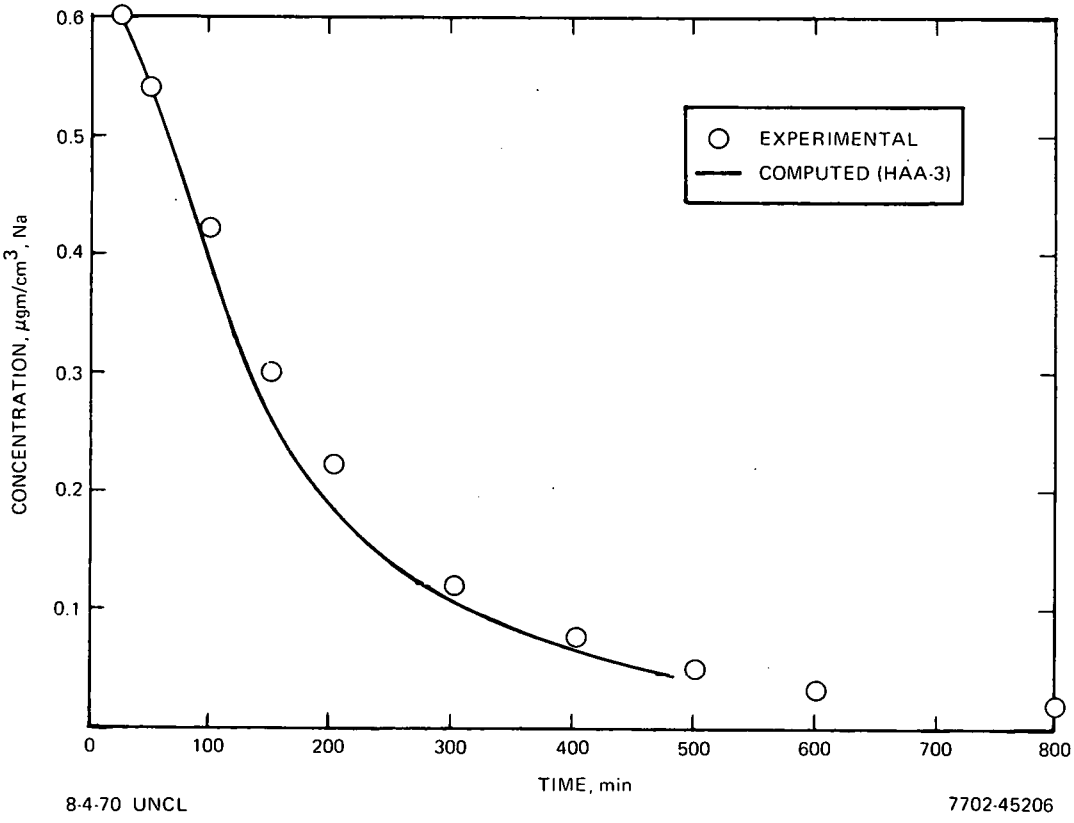

Figure 25. Airborne Mass Concentration for Test No. 6

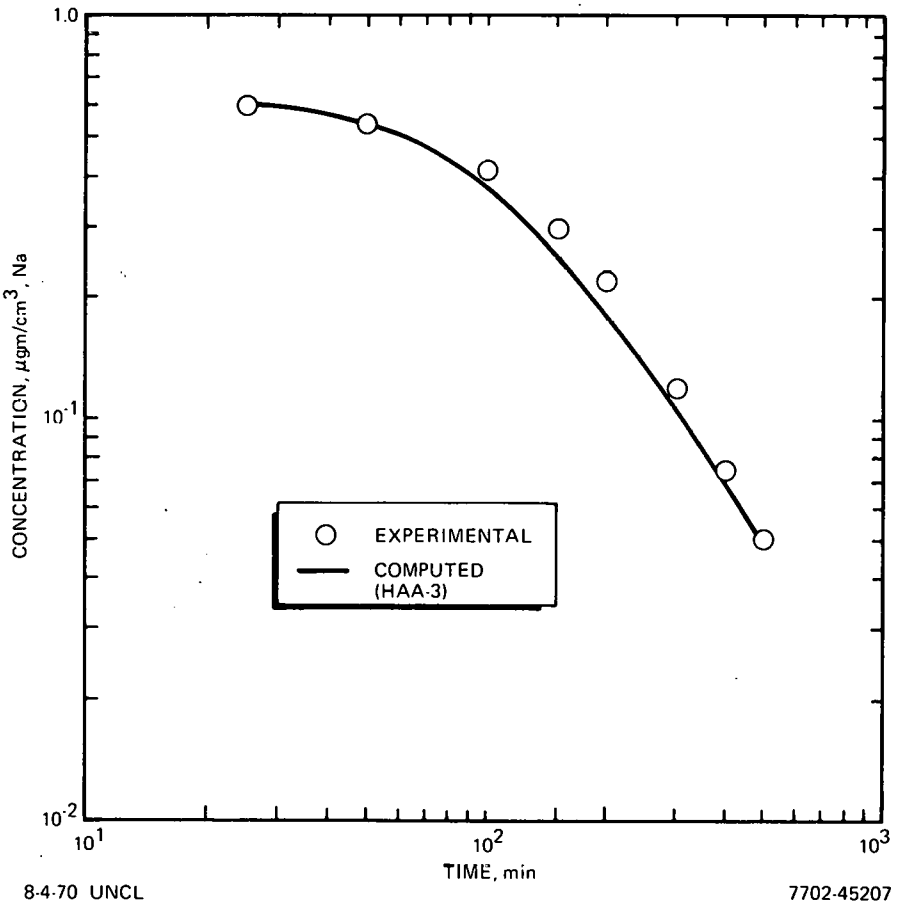

Figure 26. Airborne Mass Concentration at Extended Time for Test No. 6

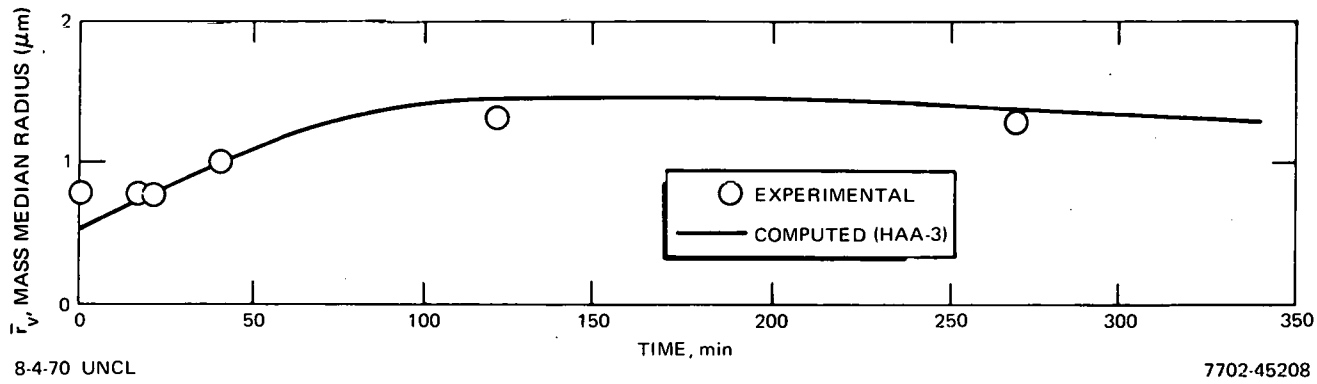

Figure 27. Median Airborne Particle Size for Test No. 6

TABLE V

CODE INPUT PARAMETER VALUES FOR SODIUM OXIDE AEROSOLS IN THE LTV

Selected Input Parameter to Simulate	Test 3	Test 4	Test 5	Test 6
M_R (gm) (Na)	8120	7800	3830	36
(lb)	17.7	17.5	8.5	0.08
C_R (μgm/cm^3) (Na)	135	130	64	0.64
(sec)	3800	3200	4200	1200
Q (μ^3/cm^3) C_R/δ_I	8×10^7	7.68×10^7	3.86×10^7	6.17×10^5
$r_v(t=0)$ (μm)	0.5	0.5	0.5	0.5
σ	2	2	2	2
α	1/4	1/4	1/4	1.0
N_o (oxide particles/cm^3)	1.3×10^9	1.3×10^9	6.4×10^8	10^7
S_o (particles/cm^3-sec)	Variable	Variable	Variable	Variable
Δ (μm)	1×10^{-5}	2×10^{-5}	2×10^{-5}	5×10^{-4}

where

M_R = mass of aerosol available for fallout and plating,

$C_R = \frac{M_R}{V}$,

τ = length of time to product M_R,

δ_I = ideal material density (grams/cc),

$\bar{r}_v$ = median radius by volume (or mass),

σ = geometric standard deviation,

$\alpha = \frac{v_e}{V_I}$ = Stoke's factor,

δ_e = effective material density; v_e = effective settling velocity,

V = volume of LTV,

$N_o = \frac{3}{4\pi} \frac{Q \exp\left(\frac{9}{2} \ln^2 \sigma\right)}{(r_v)^3}$ = initial particle concentration,

Δ = wall plating distance, and

$Q = C_R/\delta_I$, the fraction of V occupied by the released mass

D. DISCUSSION

This portion of the report has given comparisons of theory and experiment for two very different geometries (volume ratio exceeds 50). Also, the maximum released concentrations differ by a factor of 50 for the LTC and a factor of 200 for the LTV. The ability of the theory to accommodate these large differences in mass concentration and geometry is a strong indicator of the basic validity of the theory. In particular, the correct prediction of the dramatic increase in particle size in the LTV experiments has a most important implication for safety, since large sizes, which result from large released masses, mean rapid fallout will occur in the primary containment.

TABLE VI

INPUT PARAMETERS FOR LMFBR BASE CASE

Parameter	Inner Containment	Outer Containment
Mass released, (kgm)	420	
PuO_2 released, (kgm)	20	
Volume, (m^3)	5.2×10^3	3.8×10^4
Height, (m)	10.4	22.4
Ideal density, (gm/cm^3)	3.00	3.00
Leakage rate	Variable	Variable
Gas temperature, (^oK)	800	400
Gas Viscosity, Poise	3.70×10^{-4}	2.27×10^{-4}
Initial mass median radius, (μm)	0.3	Variable
Initial sigma	2.0	Variable
Collision efficiency of gravitational agglomeration	1.0	1.0
Correction factor for Stoke's settling velocity	0.33	1.0

VI. THE SENSITIVITY OF HAA-3 CODE TO VARIATIONS IN INPUT PARAMETERS

The siting requirements for the LMFBR are that the prescribed limits in 10CFR100 shall not be exceeded at the nearest point of public approach to the proposed site. Exposure to the public at this distance would be due mainly to the material which leaks from the containment and is transported to the site boundary. The amount of material which leaks has been shown to be dependent on the amount of material released during a DBA, the behavior of the resulting aerosol in both primary and secondary containment, and the leakage characteristics of both containment structures.[26]

The mass of material released in a DBA is also a function of the estimated energy release for the DBA, the leakage rate defined for a design pressure, and the pressure time history.

The behavior of the aerosol and its decrease as an airborne phase is a function of the several interacting mechanisms described earlier in the report. The effect of these mechanisms on reducing the airborne concentration and the subsequent leakage to the atmosphere is a function of a number of input parameters used in HAA-3A to describe the behavior of an aerosol. Some of these parameters, such as height and volume of the containment, leakage characteristics of the containment, mass of material released, and gas temperature, are fixed by the description of the accident. Other parameters which are less well understood can be varied by the safety analyst to study the sensitivity of the computed results to their variations. The initial particle size distribution of the released material, the efficiency of gravitational and turbulent agglomeration, and the correction to Stokes settling velocities due to nonspherical loosely packed agglomerates are of this nature.

The input parameters for the LMFBR base case are shown in Table VI. A series of HAA-3A computations were performed to determine the sensitivity of the calculations to changes in input parameters. The parameters which were varied were the input mass median radius and the magnitude of Stokes factor, the efficiency of gravitational agglomeration, and gas temperature.

Table VII compares the leaked mass as a result of these calculations. The data show that the mass of material which leaks from the outer containment is

TABLE VII

PARAMETER SENSITIVITY OF LMFBR BASE CASE

Parameter	Mass Leaked from Primary (gm)	Total Mass Leaked from Outer (gm)		Plutonium Leaked from Outer (gm)	
		2 hr	30 days	2 hr	30 days
LMFBR Base Case Stokes velocity Correction in Outer = 1.0	312.6	1.2×10^{-2}	2.1×10^{-1}	6.0×10^{-4}	1.0×10^{-2}
Initial MMR, 0.3μ Stokes Correction Factor in inner and outer = 0.33 Gravitational Collision Efficiency = 1.0	406.2	1.2×10^{-2}	6.6×10^{-1}	6.0×10^{-4}	3.3×10^{-2}
Initial MMR, 0.3μ Stokes Correction Factor in inner and outer = 0.10 Gravitational Collision Efficiency = 1.0	1.05×10^{3}	1.7×10^{-2}	1.83	8.5×10^{-4}	9.2×10^{-2}
Initial MMR, 0.3μ Stokes Correction Factor in inner and outer = 0.33 Gravitational Collision Efficiency = 0.0	5.23×10^{3}	5.6	6.2	2.8×10^{-1}	3.1×10^{-1}
Initial MMR, 0.1μ Stoke's Factors = 0.33 Efficiency = 1.0	430.9	1.3×10^{-2}	7.0×10^{-1}	6.5×10^{-4}	3.5×10^{-2}
Base case except viscosity $= 1.86\times10^{-4}$ Temperature = 300 K	242.2	7.2×10^{-3}	3.9×10^{-1}	3.6×10^{-4}	2.0×10^{-2}

insensitive to reductions in the input particle size from 0.3 to 0.1μ. As the size is increased, the mass leaked decreases for the same initial concentrations. The 2-hour value of leaked mass from the outer containment is insensitive to changes in the Stoke's correction factor from 1.0 to 0.1 but the 30-day value is inversely proportional to the magnitude: that is, small settling rates increase the leaked mass. A Stokes' correction factor of 0.33 (which is in good agreement with experiment) increases the 30-day mass leaked only by a factor of 3.0 over the base case. The effects of gas temperature are realistic.

The parameter which has the greatest effect on the mass which leaks is the absence of gravitational agglomeration. When it is assumed that there is no gravitational agglomeration (the coagulation efficiency is zero), the mass leaked at 2 hours is increased by a factor of almost 50, while the 30-day leaked mass is increased by a factor of 10. Figures 28 and 29 show the aerosol behavior for the base case (efficiency of 1) and for the case with efficiency equal to zero. An additional study of the effects of collision efficiency was made and the results are shown in Table VIII. Reduction of the efficiency from 1.0 to 0.5 increases the mass leaked by less than a factor of 2.0. It has been shown in Section V that good agreement to experimental data was obtained with an efficiency of 1.0. Even if the efficiency were reduced slightly, the effect on the leaked mass from the outer containment would be minimal.

Table IX compares the total masses leaked for a mono and a heterogeneous particle size distribution. For these calculations the containment volume was 4.25×10^9 cm^3, the height was 914 cm, the leak rate was constant at 10 vol % per day, and the gravitational efficiency was 1.0. It can be seen that if the input material is monosized and the initial concentration is constant (sigma equals 1.0), changes in the initial size of the aerosol do not significantly change the leaked mass. For heterogeneous aerosols (sigma equal to 2.0), the mass leaked is inversely proportional to the initial median size. The total mass leaked at the lower initial concentration is higher because agglomeration is not as effective as it is at the higher concentration. The aerosol remains airborne longer and allows more material to leak.

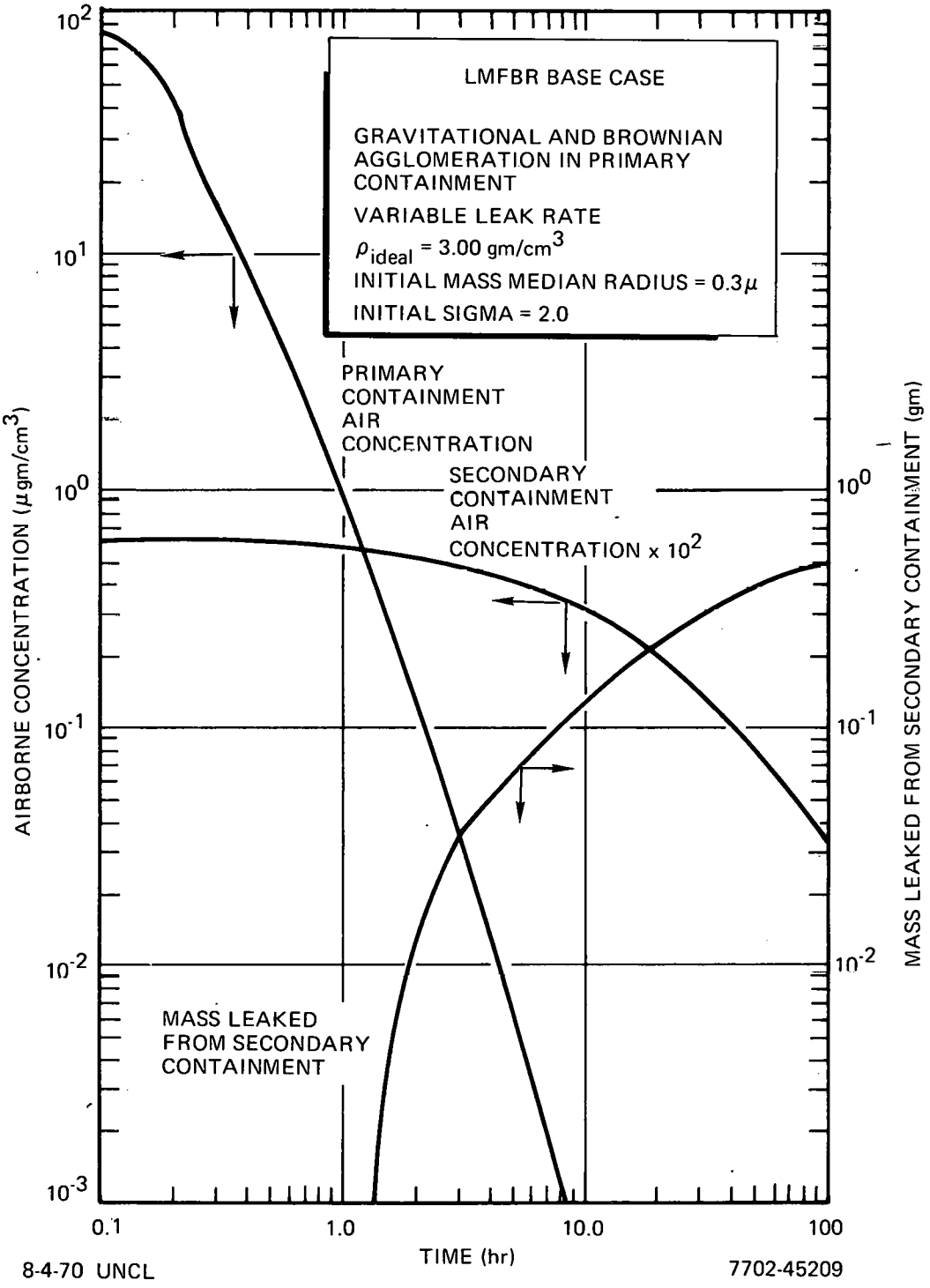

Figure 28. LMFBR Base Case with Stokes Correction Factor = 0.33 and Collision Efficiency = 1.0

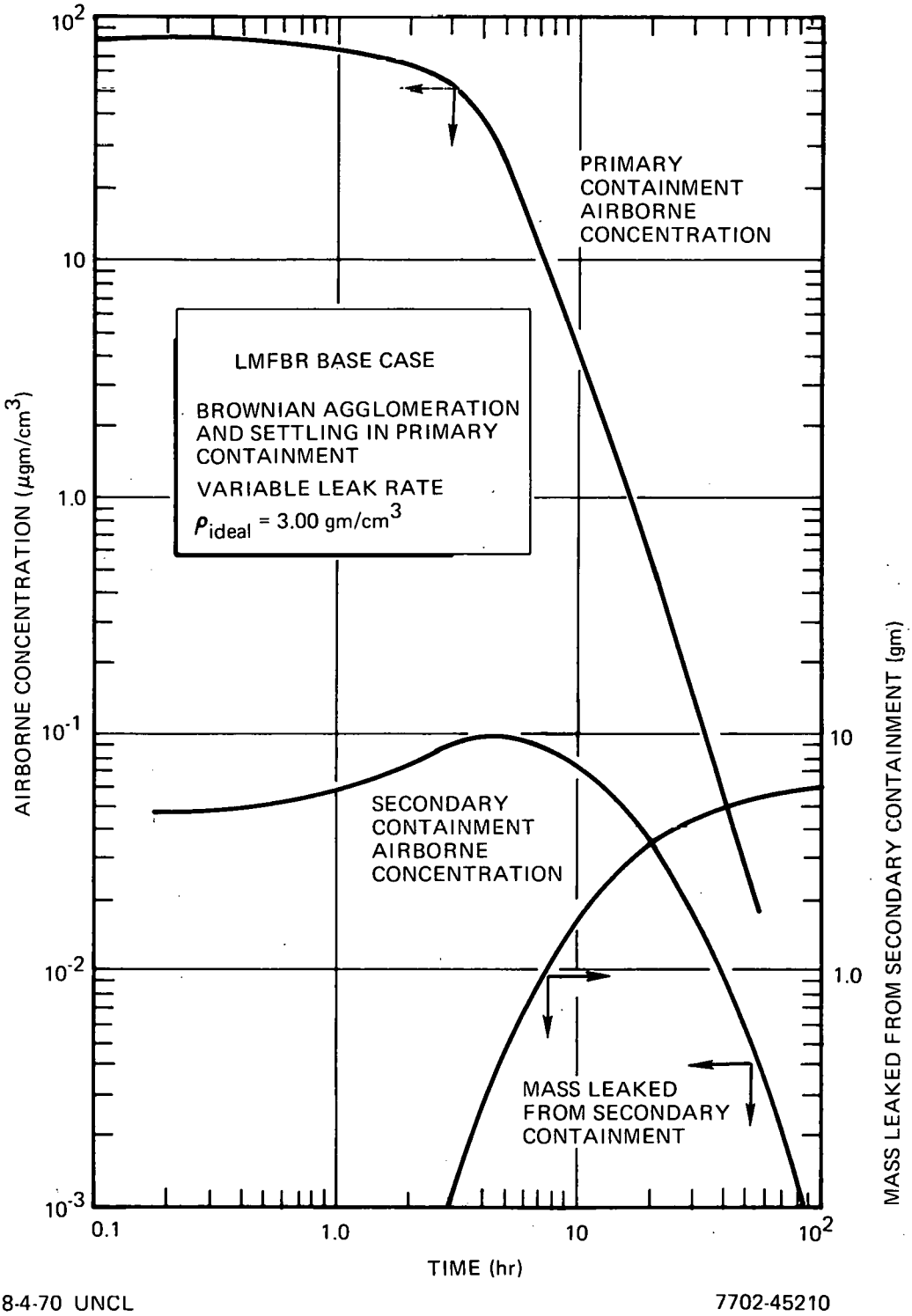

Figure 29. LMFBR Base Case with Stokes Correction Factor = 0.33 and Collision Efficiency = 0.0

TABLE VIII

EFFECTS OF COLLISION EFFICIENCY OF GRAVITATIONAL AGGLOMERATION

	Collision Eff = 1.0	Collision Eff = 0.5	Collision Eff = 0.0
Initial Conc., $\mu gm/cm^3$	235	235	235
Initial Air Conc., Half-time, sec	62.5	105	4.0×10^3
30 Day Mass Leakage, gms from Inner Containment	74.7	130	6.5×10^3
Initial Conc., $\mu gm/cm^3$	23.5	23.5	23.5
Initial Air Conc., Half-time, sec	610	1040	1.0×10^4
30 Day Mass Leakage, gms from Inner Containment	86	156	1.6×10^3

TABLE IX

EFFECTS OF INPUT PARTICLE SIZE PARAMETERS

Conc. gm/cm^3	$(\bar{r}_v)_o$	$(\sigma)_o$	ρ	Initial Air Conc. Half Time, Sec	Total Mass Leaked From Inner Containment (gm)
235	0.1	1.01	1.0	62.0	73.8
235	0.5	1.01	1.0	61.5	73.4
235	1.0	1.01	1.0	56.5	67.6
235	0.1	2.00	1.0	62.5	74.7
235	0.5	2.00	1.0	40.0	48.0
235	1.0	2.00	1.0	27.1	33.5
23.5	0.1	1.01	1.0	608	84.8
23.5	0.5	1.01	1.0	603	83.7
23.5	0.1	2.00	1.0	607	86.2
23.5	0.5	2.00	1.0	400	63.3
23.5	1.0	2.00	1.0	282	51.1

All previous safety analyses of hypothetical LMFBR accidents have been made with the assumption that an instantaneous source occurs. Calculations were made to determine the effect of different source times on the leaked mass. Table X shows these comparisons. It can be seen that increasing the source time increases the mass leaking from the inner containment to the outer and would also cause an increase in the amount of material which could leak to the atmosphere. Table X also shows the 2-hour leaked mass and the $t = \infty$ leaked mass are the same when the source time is not too long. It is unlikely that the prolonged source will have as much released mass concentration as the instantaneous source.

The calculations presented herein show the versatility of the model and how the high initial concentrations rapidly reduce the aerosol concentration which is available to leak.

If a constant released mass is assumed and the number of released particles at the time of the DBA is calculated from the ideal density (N_o = constant), then the use of a reduced Stoke's settling velocity will increase the amount of material which will leak from the containment. The increased leakage occurs because the reduced settling velocity causes the aerosol material to remain airborne longer. However, the increased residence time allows the aerosol to agglomerate to larger sizes, which in turn have greater settling velocities. The net result is an increase in the amount leaked but not as much as one would predict from the ratio of the densities. At high initial concentrations of small particles, a decrease in the Stoke's factor of 1/4 increases the mass leaked by slightly less than a factor of 3.

An evaluation of the time of occurrence of the asymptotic "self-preserving" value of $\sigma = 1.32$ has been made. It is clear that high number concentrations, and low initial sizes reach essentially self-preserving distributions which are not strong functions of the initial conditions. The computations agree with theories developed by Hidy, et al., in 1965.[14]

TABLE X

EFFECTS OF CONTINUOUS SOURCE RELEASE

	Source Time (hr)		
	0	1	4
C_R (gm/cm^3)	235.	235	235
$(\bar{r}_v)_o$	0.5	0.5	0.5
$(\sigma)_o$	2.0	2.0	2.0
Mass Leakage at two hours	48.0	480.0	446.8
Mass Leakage at $t = \infty$ gms from Inner Containment	48.0	482.7	974.0
C_R (gm/cm^3)	23.5	23.5	23.5
$(\bar{r}_v)_o$	0.5	0.5	0.5
$(\sigma)_o$	2.0	2.0	2.0
Mass Leakage at two hours	61.7	167.0	126.2
Mass Leakage at $t = \infty$ gms from Inner Containment	63.3	181.5	349.3

VII. SUMMARY AND CONCLUSIONS

A critical assessment of the AI aerosol modeling effort, as it applies to FBR design or licensing, has been conducted. The results of this effort have provided general substantiation of the basic validity of the HAA-3 aerosol model, and the justification for its use in LMFBR siting analysis.

The HAA-3 model has been successfully compared to aerosol experiments in a vessel (LTV) whose height is characteristic of the inner containment system. HAA-3 was able to provide a good fit in the LTV tests to four time-dependent quantities with only one adjustable parameter. However, the HAA-3 model has not as yet been tested with mixtures of UO_2, Na_2O, and fission products for the inner containment system (or LTV).

Based on the good agreement of the model predictions with the behavior of Na_2O particulates, HAA-3 can be applied with confidence to the site analysis of the current designs of LMFBR's since all agglomeration takes place in the inner containment system and only settling occurs in the outer containment before leakage to the atmosphere. Under these conditions HAA-3 provides a substantially conservative prediction of particulate release to the atmosphere.

Further substantiation of some of the parameters used in HAA-3 is, however, recommended. In particular, the terms for efficiency of gravitational agglomeration of nonspherical open network particles, and the corrections to the Stoke's settling velocity due to the loose packing of the particles which compose the agglomerate need further experimentation and analysis. In addition, the turbulence energy available to assist agglomeration needs to be measured for a variety of experimental situations to determine if terms which account for turbulent agglomeration should be incorporated in the present model, or if the present neglect of these terms is justified.

A high level of confidence in the model for predicting the radioactive aerosol leakage source term for siting analysis is obtained from a detailed evaluation of (1) uncertainties in aerosol parameters as applied to DBA conditions, and (2) the effect of these uncertainties on site safety analysis.

REFERENCES

1. Smoluchowski, M., Physik. Z., 17, 557 (1916)
2. Smoluchowski, M., Physik. Chem., 92, 129 (1917)
3. Smoluchowski, M., Z.f. Physik. Chem. 92, 137 (1918)
4. Müller, H., Kolloid Chem. Beih., 26, 257 (1928)
5. Müller, H., Kolloid Chem. Beih., 27, 223 (1928)
6. Zebel, G., Kolloid-Z., 156, 102 (1958)
7. Schumann, T. E. W., Q. J. Roy. Met. Soc. 66, 195 (1940)
8. Houghton, H. G., and Radford, W. H., Pap. Phys. Ocean Met., 6, No. 4 (1938)
9. Melzak, Z. A., Q. Applied Math., 11, 231 (1953)
10. Marshall, J. S., and Palmer, W. McK, J. Meteor. 5, 4, 165 (1948)
11. Saffman, P. G., and Turner, J. S., J. Fluid Mech., 1, 16 (1956)
12. Friedlander, S. K., J. Meteor., 17, 479 (1960)
    Friedlander, S. K., J. Meteor., 18, 753 (1961)
    Friedlander, S. K., "The Similarity Theory of the Particle Size Distribution of the Atmospheric Aerosols," Paper presented at the First National Symposium on Aerosols, Prague (1962)
    Swift, D. L., and Friedlander, S. K., J. Colloid Sci. 19, 621 (1964)
    Friedlander, S. K., and Wang, C. S., J. Colloid and Interface Sci. 22, 126 (1966)
    Wang, C. S., and Friedlander, S. K., J. Colloid and Interface Sci. 24, 170 (1967)
13. Todes, O. M., Collection: Problems in Kinetics and Catalysis, VII, Izd-vo AN SSSR (1949) (Referred to by Martynov and Bakanov in Reference 18)
14. Hidy, G. M., J. Colloid Sci. 20, 123 (1965)
    Hidy, G. M., and Brock, J. R., J. Colloid Sci. 20, 477 (1965)
    Hidy, G. M., and Lilly, D. K., J. Colloid Sci. 20, 867 (1965)
15. Takahashi, K., and Kasahara, M., Atmos. Environment 2, 441 (1968)

16. Rosinski, J., Werle, D., and Nagamoto, C. T., J. Colloid Sci. 17 (8), 703 (1962)

17. McLeod, J. G., Quart. J. Math. (Oxford) (2), 13, 119 (1962)

McLeod, J. G., Quart. J. Math. (Oxford) (2), 13, 193 (1962)

McLeod, J. G., Quart. J. Math. (Oxford) (2), 13, 283 (1962)

McLeod, J. G., Proc. London Math. Soc. (3), 14, 445 (1964)

18. Martynov, G. A., and Bakanov, S. P., Research in Surface Forces, edited by V. Deryagin, p. 182 Consultant Bureau, New York (1961)

19. Fair, G. M., and Gemmell, R. S., J. Colloid Sci. 19, 360 (1964)

20. Camp, T. R., Trans. Am. Soc. Civil Engrg. 120, 1 (1965)

21. Huebsch, I. O., "Relative Motion and Coagulation of Particles in a Turbulent Gas," Navy Report Number USNRDL-TR-67-49 (1967)

Huebsch, I. O., Giallanza, F. V., and Galant, D. C., "Water-Surface-Burst Fallout Model: Computer Programs," Navy Report Number USNRDL-TR-68-61 (1968)

Huebsch, I. O., "The Formation, Dispersion and Deposition of Fallout Particles from Sea-Water-Surface Nuclear Explosions," Navy Report Number NRDL-TR-68-141 (1968)

22. Spiegler, P., Morgan, J. G., Greenfield, M. A., and Koontz, R. L., "Solutions of a General Equation for the Coagulation of Heterogeneous Aerosols," NAA-SR-11997, Vol. I (1967)

23. Hausknecht, D. F., and Greenfield, M. A., Trans. Am. Nucl. Soc. 10, 690 (1967)

24. "Annual Technical Progress Report, AEC Unclassified Programs, Fiscal Year 1967," NAA-SR-12492 (1967)

25. Koontz, R. L., Nelson, C. T., Baurmash, L., and Johnson, R. P., Trans. Am. Nucl. Soc. 12 (1) 331 (1969)

26. Koontz, R. L., and Baurmash, L., "Analysis of Aerosol Behavior for FFTF Hypothetical Accidents," AI-69-MEMO-95 (October 28,1969)

27. Castleman, A. W., Horn, F. L., and Lindauer, G. C., "On the Behavior of Aerosols Under Fast Reactor Accident Conditions," BNL-14070 (1969)

28. Zebel, G., "Coagulation of Aerosols," pp 34-36, in Aerosol Science, C. N. Davies, ed., Academic Press (1966)

29. Whytlaw-Gray, R., and Patterson, H. S., Smoke: Study of Aerosol Disperse Systems, Edward Arnold and Co., London (1932)

30. Whitby, K. T., and Liu, B. Y. H., "The Electrical Behavior of Aerosols," p. 73 in Aerosol Science, C. N. Davies, ed., Academic Press (1966)

31. Cohen, E. R., and Vaughan, E. V., "Approximate Solution of the Equations for Aerosol Agglomeration," AI-AEC-12965 (to be published)

32. Fuchs, N. A., The Mechanics of Aerosols, p. 40, Pergamon Press (1968)

33. Ibid, p. 18

34. Stober, W., Berner, A., and Blasche, R., "The Aerodynamic Diameter of Aggregates of Uniform Spheres," J. Coll. Inter. Sci., 29, 710 (1969)

35. Lane, W. R., and Stone, B. R. D., "Structure and Density of Particulate Aggregates," Int. Conf. on Mechanisms of Corrosion by Fuel Impurities, Butterworths (1963)

36. Johnstone, H. F., "The Agglomeration of Solid Aerosol Particles," COO-1018, (March 1959)

37. Rossi and Staub, Ionization Chambers and Counters, McGraw-Hill Book Co. (1949)

38. Zebel, G., "Coagulation of Aerosols," pp 42-45, in Aerosol Science, C. N. Davies, ed., Academic Press (1966)

39. Nelson, C. T., Koontz, R. L., and Baurmash, L., Trans. Am. Nucl. Soc., 10, 698 (1967)

40. Fuchs, N. A., The Mechanics of Aerosols, p. 162, Pergamon Press (1968)

41. Sedunov, Yu. S., "The Relative Motion of Stokesian Particles in Turbulent Flow," Izv. A. N. SSSR, Ser. Geophys., (1962) (Referred to by Huebsch in Reference 21a

42. Corn, M., "Adhesion of Particles," p. 360, in Aerosol Science, C. N. Davies, ed., Academic Press (1966)

43. Fish, B. R., "Surface Contamination," Proceedings of a Symposium held at Gatlinburg, Tennessee (June 1964)

44. Greenfield, M. A., Koontz, R. L., and Hausknecht, D. F., "Characteristics of Aerosols Produced by Sodium Fires, Vol. II: Comparisons of Experiment with a General Equation for the Coagulation of Heterogeneous Aerosols," AI-AEC-12878 (1969)

45. Hubner, R. S., "An Approximate Solution to the General Equation for the Coagulation of Heterogeneous Aerosols," AI-AEC-MEMO-12880 (1969)

46. Hubner, R. S., "Aerosol Stirred Settling Model, Code Version 5 (SSM-5)," (to be published)